HEP'97 #589
Submitted to Pa 11, 13
Pl 9, 15,17

DELPHI 97-119 CONF 101
20 July, 1997

Search for R-Parity violating effects at $\sqrt{s}$ 161 and 172 GeV

Preliminary
DELPHI Collaboration

Y. Arnoud[5], R. Barbier[4], C. Bérat[5], M. Besançon[1], M. Boonekamp[1], K. Cieslik[3], S. Fichet[7], P. Gris[1], S. Katsanevas[4], P. Kluit[8], S. Lola[2], A. Onofre[6], H. Palka[3], Th.D. Papadopoulou[9], M. Pimenta[6], R. Nicolaidou[5], F. Richard[10], G. Sajot [5], N. Vassilopoulos[11], M. Witek[3]
CEA/DAPNIA/SPP[1] Saclay, CERN[2], INP[3] Krakow, IPN[4] Lyon, ISN[5] Grenoble, LIP[6] Lisboa, LPNHE[7] Paris, NIKHEF[8] Amsterdam, NTU[9] Athens, Orsay[10] Paris, Oxford[11] University

Abstract

Searches for charginos, neutralinos and sleptons in e^+e^- collisions at center-of-mass energies of 161 and 172 GeV have been performed on DELPHI data, under the assumptions that R-Parity is not conserved and that the dominant R-Parity violating couplings involve only leptonic or only quark fields. Particular emphasis is given in decays involving, the minimally constrained by low-energy studies, third generation couplings including τ's and b quarks in the decay products. Squark decays are also studied for the same energies assuming that the dominant R-Parity violating couplings involve a mixture of leptonic and quark fields. In the above studies, it is assumed that the strength of the couplings is such that the lifetimes can be neglected. These searches are used to constraint domains of the parameter space, previously explored under the assumption of R-Parity conservation. Further, the single sparticle production, possible when R-parity is not conserved, is studied. In particular the single squark production and the production of a sneutrino resonance in the s-channel decaying to a single chargino and a charged lepton are studied. Finally, DELPHI analysis of the indirect effects of particles carrying lepton and quark numbers, exchanged in the t-channel, are interpreted in terms of R-parity violating squark exchanges.

Paper submitted to HEP'97 Conference
Jerusalem, August 19-26

1 Introduction

1.1 The R-Parity violating Lagrangian

During the last years, supersymmetry has been used extensively to chart the map of possible physics beyond the standard model (SM). This symmetry predicts the existence of additional particles, which differ from their standard model partners by a half-integer spin. The masses and couplings of the new supersymmetric states are related by the symmetry to those of the SM states. The simplest model available is the Minimal Supersymmetric Standard Model (MSSM) [1], which contains the minimal number of new particles and interactions that are consistent with the SM gauge group. In this framework, many theoretical questions of unified theories such as the hierarchy problem and the unification of couplings, may be successfully addressed.

However, the facts that a) no such partners, degenerate in mass with the known particles have been found to date, and b) many measurements of particle properties (e.g the proton lifetime) could be endangered by the virtual exchange of this new class of particles, imposes two major modifications to the symmetric picture:

- The symmetry can not be exact, but has to be broken in a way that its nice predictions are still valid. In this case, the spectrum of supersymmetric partners is determined by a "soft" supersymmetry breaking mechanism. The details of the theory, as well as the phenomenological signatures, depend on the assumption of the supersymmetry breaking mechanism (e.g gravity or gauge mediated supersymmetry breaking).
- The standard particle parameters are protected by a new multiplicatively conserved quantum number, R-Parity R_p [2]. This number assures the conservation of the leptonic (L) and baryonic (B) numbers or, more specifically, the conservation of the so-called $(B-L)$ symmetry. It can be expressed in the form $R_p = (-)^{(2S+3B+L)}$ for a particle with spin S: it is even for standard particles and Higgs bosons and odd for their supersymmetric partners. The phenomenological consequences of the conservation of R-parity can be summarized in two points: a) supersymmetric particles are produced in pairs and b) the Lightest Supersymmetric Particle (the LSP) is stable.

Most studies at LEP apart from a few exceptions [3], have searched for supersymmetric particles and have put limits on the supersymmetric spectrum assuming R-Parity conservation. Nevertheless, the supersymmetric Lagrangian derived within the MSSM, possesses a more general expression when one includes the following supersymmetric invariant terms:

$$\lambda_{ijk} L_i L_j \bar{E}_k + \lambda'_{ijk} L_i Q_j \bar{D}_k + \lambda''_{ijk} \bar{U}_i \bar{D}_j \bar{D}_k \qquad (1)$$

where L and E (Q and U, D) denote the left-handed component of lepton doublet and antilepton singlet (quark doublet and antiquark singlet) chiral superfields respectively. The λ_{ijk}, λ'_{ijk} and λ''_{ijk} are new Yukawa couplings, where i, j and k are family indices going from 1 to 3. The terms proportional to λ and λ' violate L explicitly, whereas the term with a λ'' coupling, violates B explicitly. In order to avoid an unacceptably large amplitude for proton decay through squark exchange, it is sufficient to assume that certain "dangerous" lepton and baryon number violating couplings that would generate such a process, are not simultaneously present in the low energy Lagrangian. It has been shown in the literature, that as a result of symmetries, it is indeed possible to have large R-parity violating couplings in a way that the proton stability is maintained [4]. The simplest (and most conservative) assumption that one can make, is that one R-parity violating coupling is dominant. In tables 1, 3 and 8, we report the existing limits from virtual exchange of R-Parity violating sparticles under this assumption [5, 6][1].

Due to $SU(2)$ invariance, there are only 9 allowed λ terms i.e. all combinations of i, j and k going from 1 to 3 with $i \neq j$. There are 27 allowed λ' terms i.e. all combinations of i, j and k going from 1 to 3. Finally, from $SU(3)$ invariance, there are only 9 λ'' allowed terms i.e. all combinations of i, j and k going from 1 to 3 with $j \neq k$. This amounts in total to 45 new possible terms in the Lagrangian, leading to a large but manageable diversity of the possible experimental signatures and topologies [5, 9, 10, 11].

One of the main phenomenological consequence of the R-Parity violating models ($\not{R}_p$) is the decay of the LSP. While in the context of R-Parity conserving models (R_p) the LSP candidates have to be neutral[2] for cosmological reasons, in $\not{R}_p$ models any particle can be the LSP (although if one makes the additional assumption of universality for superparticle masses at the GUT scale, the possible LSP candidates are more constrained). The absence of a model-independent prediction for the supersymmetric spectrum, greatly enlarges the parameter space to be searched in the case of these models.

In this paper we will study three possible manifestations of R-Parity violation in an e^+e^- collider i.e. pair production of sparticles and subsequent decay through R-Parity violating couplings, R-Parity violating single production of sparticles and finally indirect effects on standard particle production cross section and asymmetries, through a R-parity violating exchange in the t channel.

1.2 Decays

We can distinguish the $\not{R}_p$ decays of the supersymmetric particles in 2 categories:

- **direct $\not{R}_p$ decays**. The sparticle decays directly or via a virtual exchange to standard particles through an $\not{R}_p$ vertex. This is always the case when the sparticle is the LSP. If e.g the $\tilde{\nu}$ is the LSP, it can decay directly to a pair of fermions through the above mentioned $\not{R}_p$ terms. If on the other hand the lightest neutralino $\tilde{\chi}^o_1$ is the LSP, then it can decay into a fermion virtual-sfermion pair with the subsequent decay of the sfermion to standard fermions via the R-parity violating terms (see figures 1 and 2).
- **indirect $\not{R}_p$ (or cascade) decays**. The sparticle first decays through an R_p -conserving vertex to an on-shell sparticle which then decays through a $\not{R}_p$ vertex. This mode usually dominates when there is enough phase space between the "mother" and the "daughter" sparticle. As a rule of thumb, when the difference of masses between these 2 sparticles is larger than 5-10 GeV the **indirect** mode tends to dominate. An exception to this can be the light stop decay, whose R_p decay is naturally suppressed. A typical example of **indirect** decay is the R_p decay $\tilde{\chi}^+_1 \rightarrow \tilde{\chi}^0_1 + W^{*+}$ and the subsequent decay of $\tilde{\chi}^0_1$ through the $\not{R}_p$ couplings. In the case of λ'' dominance, the **direct** $\tilde{\chi}^+_1$ decay has a signature of 3 jets, while the **indirect** would give either 5 jets or 3 jets + 1 lepton + missing energy, depending on the decay modes of W^* (see fig 3)

Given the existing experimental limits on the couplings λ, the two decay modes may compete at regions with some form of degeneracy between mother and daughter sparticles. In this paper, we will mainly study the signatures of the **direct** $\not{R}_p$ decays[3]. The **indirect** decays

[1] We do not refer to cosmological constraints on R-parity violating interactions [7] as they can be avoided in various schemes, such as electroweak baryogenesis [8]

[2] e.g the $\tilde{\chi}^0_1$ or the $\tilde{\nu}$ for gravity mediated supersymmetry breaking models

[3] In what follows we use the nomenclature direct and indirect decays to denote direct $\not{R}_p$ and indirect $\not{R}_p$ decays

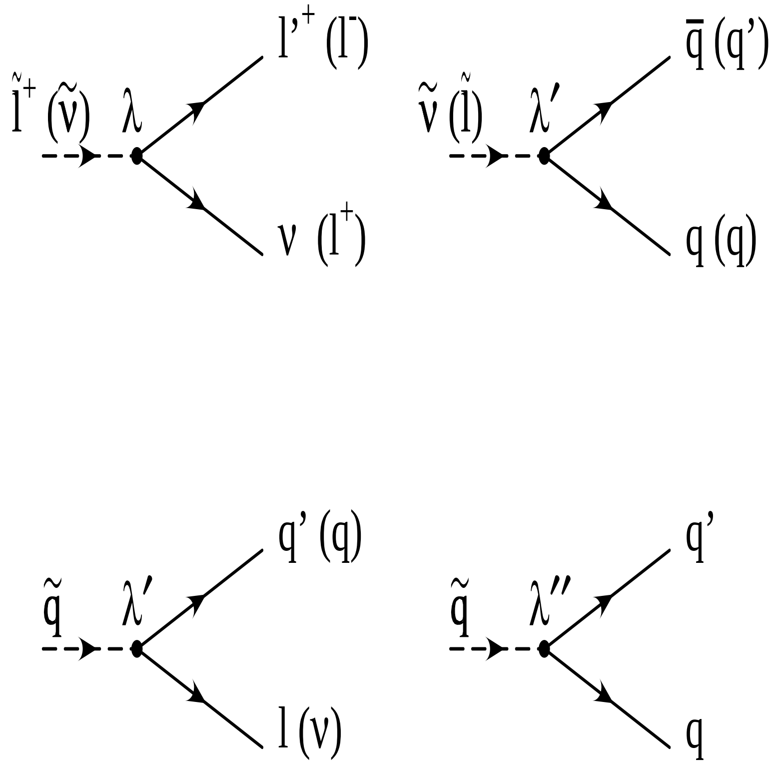

Figure 1: $\not{R}_p$ decays of sfermions

will be studied only insofar as their effect simply softens a **direct** topology, or fall into topologies covered by R_p searches. We leave the detailed study of the **indirect** decays for a later publication.

The requirement that the sparticle decays through **direct** decay within the detector (typically within 1 m) translates :

- for a sfermion e.g the $\tilde{\nu}$ to:

$$\lambda^2 \ (or\ 3\lambda'^2) \ \geq \beta\gamma \ (GeV/m_{\tilde{\nu}}) \times 10^{-14}, \tag{2}$$

  where $\beta\gamma = \sqrt{s/(4m_{\tilde{\nu}}^2) - 1}$ is the appropriate sneutrino Lorentz factor and λ (or λ') denotes the coupling of the dominant decay process to leptons or quarks. For the energies and masses of present interest, this implies very weak lower bounds $\lambda, \lambda' \gg 10^{-8}$ on the dominant couplings.

- and for a gaugino e.g the $\tilde{\chi}_1^0$ into [10]:

$$\lambda^2 \ (or\ 3\lambda'^2) \ \geq 25\beta\gamma \ (m_{\tilde{f}})^4 \ (m_{\tilde{\chi}_1^0})^{-5} \times 10^{-14}, \tag{3}$$

  where λ denotes the dominant $\not{R}_p$ coupling, $m_{\tilde{\chi}_1^0}$ and $\tilde{m}_f$ are the masses of $\tilde{\chi}_1^0$ and the dominant exchanged sfermion (in GeV), while $\beta\gamma = \sqrt{s/(4m_{\tilde{\chi}_1^0}^2) - 1}$ is the appropriate Lorenz factor for $\tilde{\chi}_1^0$. For typical values of present interest $m_{\tilde{\chi}_1^0} \sim 50$, $\tilde{m}_f \sim 100$, $\beta\gamma \sim 1$, this gives a very weak lower bound $\lambda \geq 3 \times 10^{-6}$.

For values of λ between 10^{-5} and 10^{-6} for the neutralinos/charginos and 10^{-7}-10^{-8} for the sfermions, the decays appear as displaced vertices in the detector. For weaker values of λ the $\not{R}_p$ signatures become indistinguishable from the R_p ones. Very low mass neutralinos decay outside the detector even for relatively high λ values.

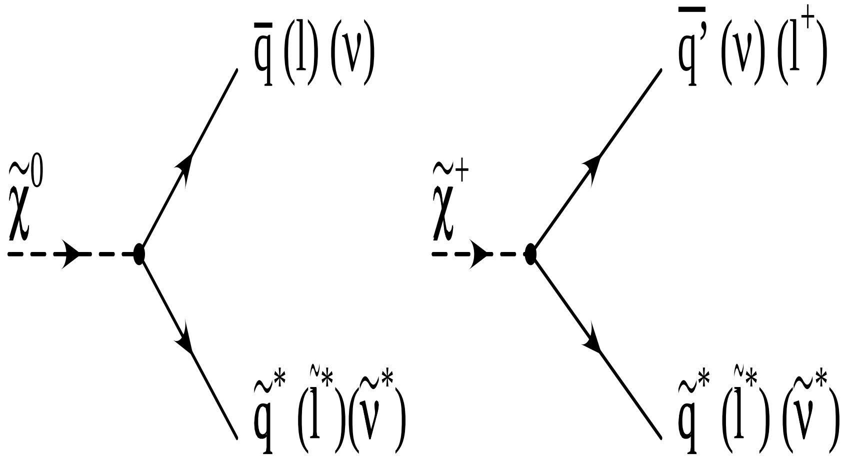

Figure 2: $\not R_p$ decays of charginos and neutralinos

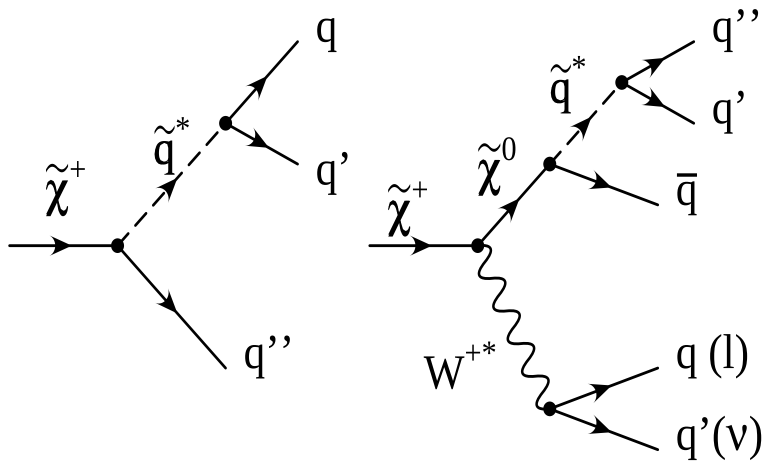

Figure 3: Direct (left) and indirect (right) $\not R_p$ decays of a chargino.

A further complication arises when λ'' or λ' are involved and the decay lifetimes to quarks become larger than the hadronization ones. Then the system hadronizes into a squark hadron before decay and all the ambiguities in the modelization of the R_p $\tilde{t}$ decay become relevant for the $\not R_p$ decays.

1.3 Production

- **Pair production of gauginos and sfermions**. It occurs through R_p couplings determined by the MSSM model parameters. The new couplings λ do not enter into the production process. They only affect the decay. As long as they are strong enough to permit a sparticle decay close to the vertex, they play a minor role in the sensitivity of detection. They are studied in sections 3, 4 and 5 corresponding to 3 distinctive signatures: leptonic, semileptonic and multi-jet hadronic.

More specifically we have searched for[4]:

- **leptonic topologies** (λ dominance)
  - $e^+e^- \to \tilde{\chi}_i^0\tilde{\chi}_i^0 \to 4\ l + Emiss$
  - $e^+e^- \to \tilde{\chi}_i^+\tilde{\chi}_i^- \to 6\ l, 4\ l + Emiss$ or $2\ l + Emiss$
  - $e^+e^- \to \tilde{\nu}\tilde{\nu} \to 4\ l$
  - $e^+e^- \to \tilde{l}^+\tilde{l}^- \to 2\ l + Emiss$
- **"semi-leptonic" topologies** (λ' dominance)
  - $e^+e^- \to \tilde{\chi}_i^0\tilde{\chi}_i^0(\tilde{\chi}_i^+\tilde{\chi}_i^-) \to 2\ l + 4\ jets$ or $4\ jets + Emiss$
  - $e^+e^- \to \tilde{t}\tilde{\bar{t}}(\tilde{b}\tilde{\bar{b}}) \to 2\ l + 2\ jets$ for direct decays and for indirect decays via $\tilde{\chi}_i^0$ 6 $jets + Emiss$ or $2\ l + 6\ jets$
- **multijet hadronic topologies** (λ'' and λ' dominance)
  - $e^+e^- \to \tilde{\chi}_i^0\tilde{\chi}_i^0(\tilde{\chi}_i^+\tilde{\chi}_i^-) \to 6\ jets$ (λ'' dominance)
  - $e^+e^- \to \tilde{t}\tilde{\bar{t}}(\tilde{b}\tilde{\bar{b}}) \to 4\ jets$ (λ'' dominance)
  - $e^+e^- \to \tilde{\nu}\tilde{\nu}(\tilde{e}^+\tilde{e}^-) \to 4\ jets$ (λ' dominance)

This is not a fully exhaustive list, since the complications of the cascade decays and the interplay of direct and indirect decays will tend to alter the number of leptons, jets and missing energy. We simulate both direct and cascade decays and accept the events that fulfill the general search criteria.

- **Single production of squarks and sleptons.** The search for manifestations of R-Parity violation can be extended to masses $\sim$ E$_{CM}$, provided we introduce at least one $\not{R}_p$ vertex in the production. The single production processes are of 2 types:
  - **single squark production** through the interaction of a quark (contained in a radiated "resolved" gamma from one of the incoming particles (e^+ or e^-) [12] (see fig. 4)

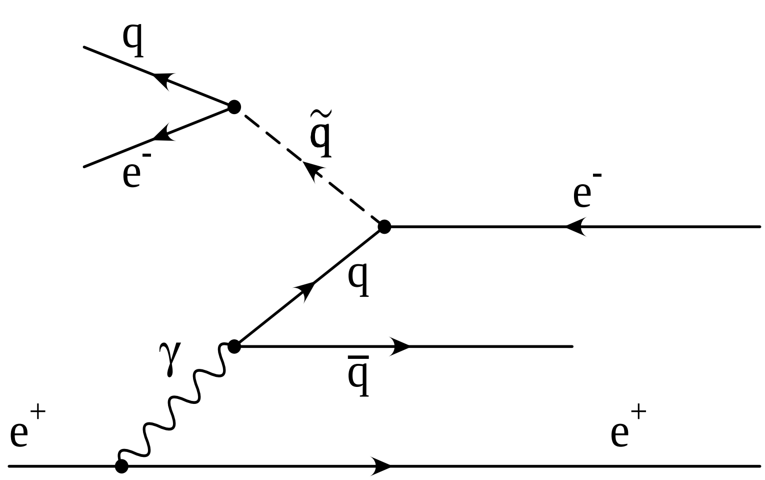

Figure 4: Single squark production

In this case as well, the direct and indirect decays respectively give:

[4] In what follows l denotes charged leptons

    - a striking signature eq of a single lepton opposite a hadronic jet, with a resonant mass, or νq missing energy and a hadronic jet, equally resonant.
    - a R_p decay to $q\tilde{\chi}_1^0$ or $q'\tilde{\chi}_1^+$, giving a final topology where a jet is opposite 2 jets and a lepton or 2 jets and missing energy.
  - **$\tilde{\nu}_\mu$ or $\tilde{\nu}_\tau$ resonant production** in the s channel through the operators λ_{121} and λ_{131} (see fig 5).

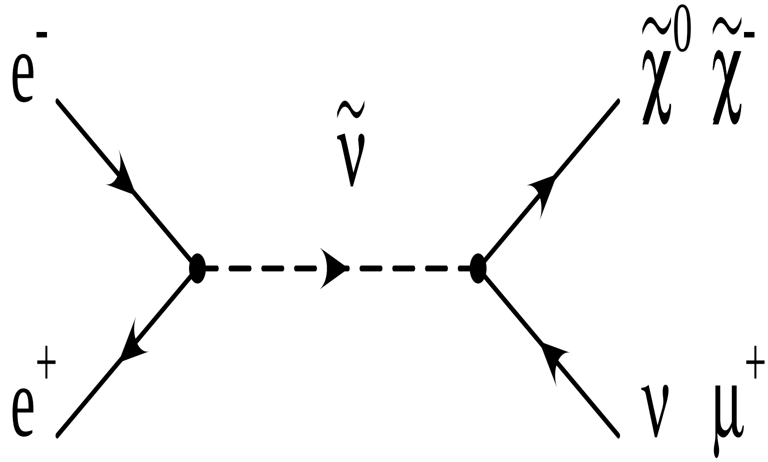

Figure 5: $\not{R}_p$ sneutrino resonance production, and decay to R_p permitted channels

  We can have 2 possible decay modes:

    - **indirect** decays when the mass of $\tilde{\chi}_1^0$ and/or $\tilde{\chi}_1^+$ is smaller than the mass of the $\tilde{\nu}$ so that the indirect R_p decay dominates. The $\tilde{\nu}$ decays first to $\nu\tilde{\chi}_1^0$ [5, 13] or $\mu^-(\tau^-)\tilde{\chi}_1^+$ [13], giving a final signature of 2 or 4 leptons with or without missing energy.
    - **direct** decays when the $\tilde{\chi}_1^0$ and or $\tilde{\chi}_1^+$ have a mass equal or larger than the mass of the $\tilde{\nu}$. The $\tilde{\nu}$ decays either through the dominant operators responsible for its production, or through any other. The R-Parity violation, will manifest itself through:
      - deviations of the R_b or some other R_q value from the SM,
      - deviations of the R_e value from the SM,
      - generational lepton number violating processes.

  This will be the subject of section 6.

- **Indirect effects on the SM cross sections and asymmetries.** Finally the t channel exchange of a squark (or slepton) can in principle give access to squarks (slepton) masses well beyond the E_{CM} energies. Deviations of the SM cross-sections and asymmetries are studied in section 7 as a means of setting new limits to $\not{R}_p$ couplings, for high sfermion masses beyond the kinematical limits of double or single sfermion production.

2 Data samples and Background Simulation

The data used in this analysis were recorded in 1996 at center-of-mass energies of 161 GeV and 172 GeV. The corresponding integrated luminosities were 9.7 pb^{-1} and 10.0 pb^{-1}, respectively. A detailed description of the DELPHI detector, of the triggering conditions and of the readout chain can be found in reference [17].

The effects of the experimental resolution, both on the signals and on the backgrounds, were studied by generating Monte Carlo events for the SM background processes and for the possible signals and passing them through the full DELPHI simulation and reconstruction chain. Some searches used a fast simulation of the detector [18] to generate a few hundreds of points of the supersymmetric parameter space. The fast simulation has been checked against the full simulation and has been found to agree within a few %. When fast simulation is used, the efficiencies have been down-scaled with factors obtained from the comparison with full simulation.

Bhabha events, $e^+e^- \to Z\gamma$, WW, $We\nu$, ZZ, Zee, events were generated with PYTHIA [19]. In all four fermion channels, studies with the EXCALIBUR generator [20] were also performed. The two-photon ("$\gamma\gamma$") physics events were generated according to the TWOGAM [21] generator for quark channels ($\gamma\gamma$ QCD, $\gamma\gamma$ QPM, $\gamma\gamma$ VDM processes) and two-photon interactions leading to leptonic final states were generated with the Berends, Daverveldt and Kleiss program [22]. The statistics of the simulated background samples were 10-20 times the real data statistic. Most of the signals have been generated with SUSYGEN 2.17 [23], apart from the stop and sbottom generation where a specific generator has been used[5].

3 Leptonic topologies

Measurements on weak processes at low energies provide strong constraints on $\not{R}_p$ interactions with L violation. Limits come from universality of quark and lepton couplings to W bosons, $\nu_\mu-$ e scattering, forward backward asymmetry in e^+e^- collisions, atomic parity violation, and ν_e -majorana mass [24] [25]. Present experimental limits on couplings are presented in table 1.

ijk	$\lambda_{ijk} \leq$	ijk	$\lambda_{ijk} \leq$	ijk	$\lambda_{ijk} \leq$
$\lambda_{\nu_e \mu e}/\lambda_{e\nu_\mu e}(121)$	0.04	$\lambda_{\nu_e \tau e}/\lambda_{e\nu_\tau e}(131)$	0.10	$\lambda_{\nu_\mu \tau e}/\lambda_{\mu\nu_\tau e}(231)$	0.09
$\lambda_{\nu_e \mu\mu}/\lambda_{e\nu_\mu \mu}(122)$	0.04	$\lambda_{\nu_e \tau\mu}/\lambda_{e\nu_\tau \mu}(132)$	0.10	$\lambda_{\nu_\mu \tau\mu}/\lambda_{\mu\nu_\tau \mu}(232)$	0.09
$\lambda_{\nu_e \mu\tau}/\lambda_{e\nu_\mu \tau}(123)$	0.04	$\lambda_{\nu_e \tau\tau}/\lambda_{e\nu_\tau \tau}(133)$	0.003	$\lambda_{\nu_\mu \tau\tau}/\lambda_{\mu\nu_\tau \tau}(233)$	0.09

Table 1: Indirect limits on the $\not{R}_p$ couplings λ in units of ($m_{\tilde{f}}$/100 GeV), where $m_{\tilde{f}}$ is the appropriate sfermion mass.

The leptonic topologies fall in 4 categories:

- Lightest neutralino pair production leading to 4 leptons and missing energy topologies. In the MSSM, assuming GUT unification for the gaugino masses, the lowest neutralino has a smaller mass than the chargino, except for a small region with positive μ and low $\tan\beta$ where the opposite happens. For this region we can use the similar direct decay of the chargino pairs to 4 leptons and missing energy, explicited below, which is abundantly

[5] See section 4 for further details

produced and passes our cuts with substantial efficiency. A decay of the lowest mass neutralino to a sfermion LSP particle does not change the signature. It only changes the kinematics making the signal more easily distinguishable, so we can safely assume that the lowest mass neutralino will decay directly to 2 leptons and missing energy ($\tilde{\chi}_1^0 \to ll\nu$).

- The chargino pair production leads to a series of distinctive topologies. Apart from cases of extreme degeneracy between the chargino and the neutralino (e.g low μ high M_2 regions), the chargino decay to the lowest mass neutralino plus an off-shell W is dominant in practically all the phase space, apart from

  In these special cases of extreme degeneracy, the chargino decays directly to either 1 lepton and 2 neutrinos, or 3 leptons ($\tilde{\chi}_1^+ \to \nu l^+ \nu$ or $\tilde{\chi}_1^+ \to l^+ l^- l^+$). When the chargino is pair produced, the mixture of these 2 possible (extreme degeneracy scheme) decays will give 2 or 4 leptons and missing energy or 6 leptons and no missing energy. The signature of 4 leptons and missing energy is identical to the neutralino direct decay. The striking signature of 6 leptons is also searched for. The search of the 2 lepton topology is covered by the R_p searches of two acoplanar leptons[6].

  In the rest of the parameter space the chargino decays indirectly giving either 3 leptons and missing energy or 2 leptons and 2 jets, following the branching ratios of the off-shell W. This will give either 6 leptons and missing energy, or 4-5 leptons, missing energy and jets. The first topology is again the same as the one of the neutralino direct decay. The second is similar to a few topologies characteristic of a λ' dominated decay, analyzed in the next section. It will be studied in a later publication. Similar arguments hold for the second neutralino direct and indirect decay.

- The sneutrino pair production leads to a topology of 4 leptons and no missing energy, when direct decays are dominant, since each sneutrino decays directly to 2 leptons ($\tilde{\nu} \to l^+ l^-$). This analysis though it exhibits similarities to the neutralino one, in the selection of candidates, differs by the fact that there is no missing energy and that one has the possibility to reconstruct the candidates mass. The indirect decay $\tilde{\nu} \to \nu \tilde{\chi}_1^0 \to \nu l^+ l^- \nu$ dominates when kinematically available and λ is below presently constrained limits. The pair production of the indirect decay gives thus a signal very similar to the one of the neutralino search. We used the combination of the 2 analyses (multi-leptons + missing energy and 4 leptons and no missing energy) to perform a model independent search.

- Charged slepton pair decays to 2 leptons and missing energy. This analysis is similar to the "standard" MSSM R-Parity conserving analysis, where the slepton decays to the corresponding slepton and a neutralino, at the kinematical limit of zero neutralino mass. We transpose here the results of R_p searches reported in [26].

To summarize in this section we present:

- the search for neutralinos, charginos and sneutrinos using the multi-leptons and missing energy topology,
- the search for sneutrinos decaying directly to 4 leptons and no missing energy and
- the reinterpretation of the R_p searches of acoplanar leptons in the context of $\not{R}_p$ models.

[6] The reinterpretation of the limits obtained in [26] in the context of $\not{R}_p$ chargino decays will be done in a future publication

3.1 Chargino and neutralino decays to multi-leptons

In the present analysis it was assumed that only one λ_{ijk} is dominant.

Two searches have been performed :

- the first assuming that λ_{122} is dominant. In this case, each $\tilde{\chi}_1^0$ can decay into $e^+\bar{\nu}_\mu\mu^-$, or $\mu^-\bar{\nu}_e\mu^+$ (and their conjugates). The corresponding final state is : missing energy, coming from the undetected neutrinos, plus $2e2\mu$ ($\approx 25\%$) or $1e3\mu$ ($\approx 50\%$) or 4μ ($\approx 25\%$). This case is the most favorable since selection depends on e and μ identification.

- the second assuming that λ_{133} is dominant. The corresponding final states are the same as for λ_{122} but with the μ replaced by τ. This case should have the worst efficiency due to the presence of several τ in the final state.

To evaluate signal efficiencies, SUSYGEN 2.17 was used to generate neutralinos ($\tilde{\chi}_1^0$,$\tilde{\chi}_2^0$) and charginos ($\tilde{\chi}_1^+$) through the processes $e^+e^- \rightarrow \tilde{\chi}_1^0\tilde{\chi}_1^0$, $\tilde{\chi}_2^0\tilde{\chi}_1^0$, $\tilde{\chi}_1^+\tilde{\chi}_1^-$. The $\tilde{\chi}_2^0$, $\tilde{\chi}_1^+$ indirect decays: $\tilde{\chi}_2^0 \rightarrow \tilde{\chi}_1^0\nu\bar{\nu}$, $\tilde{\chi}_2^0 \rightarrow \tilde{\chi}_1^0 l^+l^-$ and $\tilde{\chi}_1^+ \rightarrow \tilde{\chi}_1^0 l^+\nu$ were studied because they also lead to a multi-leptonic final state. The plane (M_2, μ) was scanned for two values of tanβ (1.5 and 30) and two values of m_0 (90 GeV/c^2 and 300 GeV/c^2). The results will be presented as exclusion contours in the plane (M_2, μ). The λ parameters have been set to their present experimental upper limits (see table 1) : $\lambda_{122} = 0.04$ and $\lambda_{133} = 0.003$.

Several points in the (M_2, μ) parameter space were generated and passed through the full DELPHI simulation in order to obtain the corresponding efficiencies. For these points, performances and efficiencies were compared with a fast simulation of the DELPHI detector. The two simulations agree very well apart from few points where the neutralino mass is very low (below 10 GeV/c^2), for which the fast simulation is around 6% more optimistic than the full simulation. The fast simulation is used to evaluate efficiencies at different points in the parameter space, taking into account the small differences between fast and full simulation as mentioned above. Of the order of one thousand points have been simulated with fast simulation.

3.1.1 λ_{122} search

Events are selected if they satisfy the following criteria:

- at least two loose muons [17] are identified in the event;
- the visible energy is greater than 40 GeV;
- the number of charged particles is in the range between 4 to 6;
- the total charged energy is greater than 30 GeV;
- an isolation criterium is imposed for the identified leptons (no other charged track in a cone of 5 degrees around the lepton);
- the missing energy is at least 15 GeV.

Effect of the cuts on the real data and on the simulated background are given in table 2.

After the cuts, no event survived, consistent with the 0.72 events expected from Standard Model processes. 70% of this background comes from the four fermion ($2e2\mu$) process. The obtained efficiencies are between 52-75% depending on the point in the (M_2, μ) plane.

3.1.2 λ_{133} search

The τ are searched as isolated particles or thin jets reconstructed using the JADE algorithm with $y_{cut} = 0.00017$ corresponding to the τ mass. In this case the missing energy is expected

Cuts	data events	Expected SM events
$E_{total} > 40$ GeV N_μ loose ≥ 2	655	652
$4 \leq N_{charged} \leq 6$	7	5
$E_{charged} \geq 30$ GeV	4	4.3
$\mid \Sigma$ Q $\mid \leq 2$	1	3
$\Theta^{min}_{lepton-track} \geq 5^o$	1	1.5
$E_{miss} > 15$ GeV	0	0.72

Table 2: Number of events remaining after each cut of the λ_{122} search on the data and on the simulated normalized background.

to be higher than in the λ_{122} case due to the presence of neutrinos coming from τ decay.
Events are selected if they satisfy the following criteria:

- at least one loose lepton is required;
- the visible energy is greater than 30 GeV;
- the number of charged particles is in the range of 4 to 8;
- the missing p_t is greater than 5 GeV/c;
- there should be no other charged track in a 5 degrees cone around the identified lepton(s);
- the missing energy is at least 60 GeV;
- The $\sqrt{s'}$ energy should not be within the Z peak $\pm$ 3.5 GeV.

Further selections based on jet properties or topologies have been applied on the remaining events :

- the number of jets in the event should be in the range 4 to 6;
- at least 4 charged jets;
- all the jets should have a polar angle in the range $20^o \leq \theta \leq 160^o$;
- at least one jet with a lepton as a leading particle;
- if leading lepton found in jet, no other charged track and no more than a neutral allowed in this jet.

No candidate event remains after the cuts with 0.9 expected events from standard background processes. The background is equally distributed to four-fermion, radiative return and WW decays to τ's. The last background becomes dominant at 172 GeV. For $\tilde{\chi}^0_1$ pair produced, efficiencies are in the range 20-37 %.

3.1.3 Results

The processes contributing to the selected final state are combined to give the exclusion contours at 95% CL in (M_2, μ). The maximum number of signal events in presence of background is given by the standard Poisson formula [27]. All the points in (M_2, μ) which satisfy the condition:

$$N \leq (\textstyle\sum_{i=1}^{i=3} \epsilon_{i,161}\sigma_{i,161})L_{161} + (\sum_{i=1}^{i=3} \epsilon_{i,172}\sigma_{i,172})L_{172},$$

where i runs for the contributing processes ($\tilde{\chi}^0_1\tilde{\chi}^0_1$, $\tilde{\chi}^0_2\tilde{\chi}^0_1$, $\tilde{\chi}^+_1\tilde{\chi}^-_1$)

DELPHI Preliminary

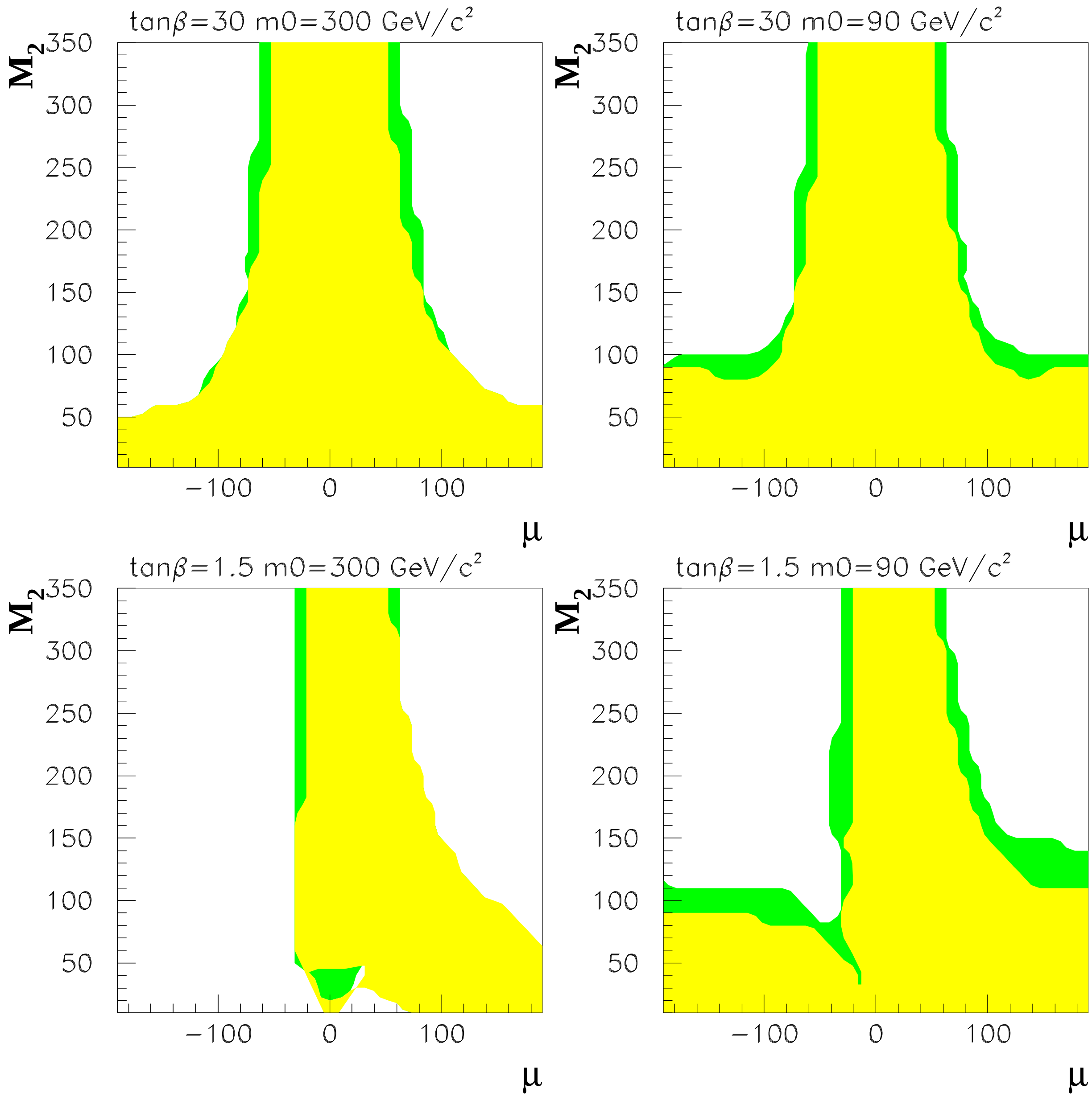

Figure 6: DELPHI PRELIMINARY : regions in (M_2, μ) excluded at 95 % C.L. for two values of tanβ and two values of m_0. The exclusion area obtained from the λ_{133} search is shown in light grey and the corresponding area for the λ_{122} search is shown in dark grey. The second exclusion area includes the first. The data collected at E_{CM} = 161 and 172 GeV, are used.

are excluded at 95% CL[7]. Using the obtained efficiencies, one deduces the exclusion contours shown on figure 6. The light grey area shows the region excluded by the λ_{133} search and the dark grey area, the region excluded by the λ_{122} search which, having a better efficiency, includes and extends the excluded region. One can consider these two searches as the most sensitive and the least sensitive cases. The other couplings must have a sensitivity lying in between these two extremes.

3.2 Sneutrino search in λ_{122} hypothesis

The cross section of sneutrino production at the center of mass of 136, 161 and 172 GeV is shown in figure 7.

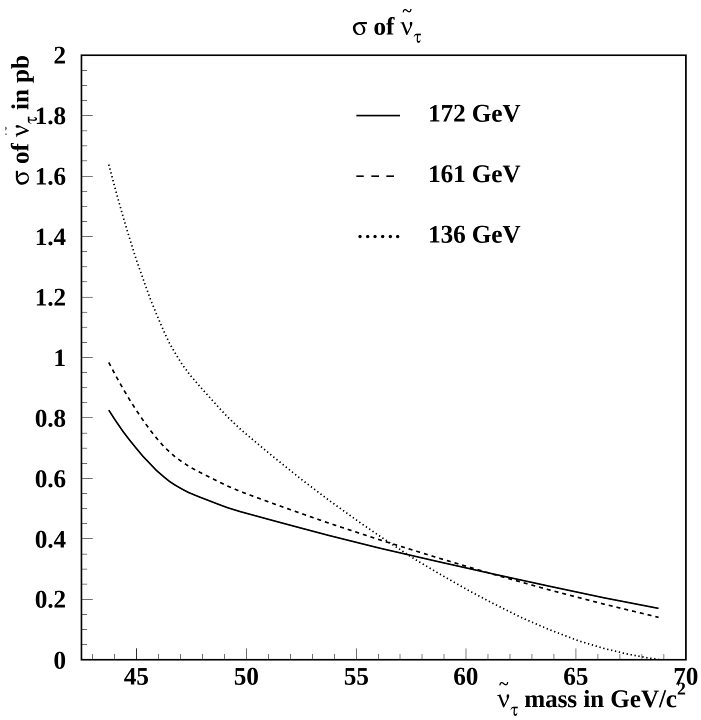

Figure 7: One generation sneutrino production cross section at different energies (the τ neutrino is shown as an example). No enhancement due to t channel exchange for the first generation is assumed.

Direct ($\tilde{\nu} \to l^+ l^-$) and indirect ($\tilde{\nu} \to \nu \tilde{\chi}_1^0$ or $\tilde{\nu} \to l^\pm \tilde{\chi}_0{}^\mp$) decays lead to different signatures.

In order to study the direct decay, events were generated with $\tilde{\nu}$ mass below that of the $\tilde{\chi}_1^0$. Events are selected if they satisfy the following criteria:

- at least two loose muons [17] are required in the event;
- the visible energy is greater than 100 GeV;
- the number of charged particles is 4;

[7] All the limits of this paper, used the above formulas to extract exclusion limits

- each loosely identified lepton should be isolated (no other charged track in a cone of 5 degrees around the lepton);
- the maximum invariant mass of any 2 leptons in the event is greater than 30 GeV/c^2.

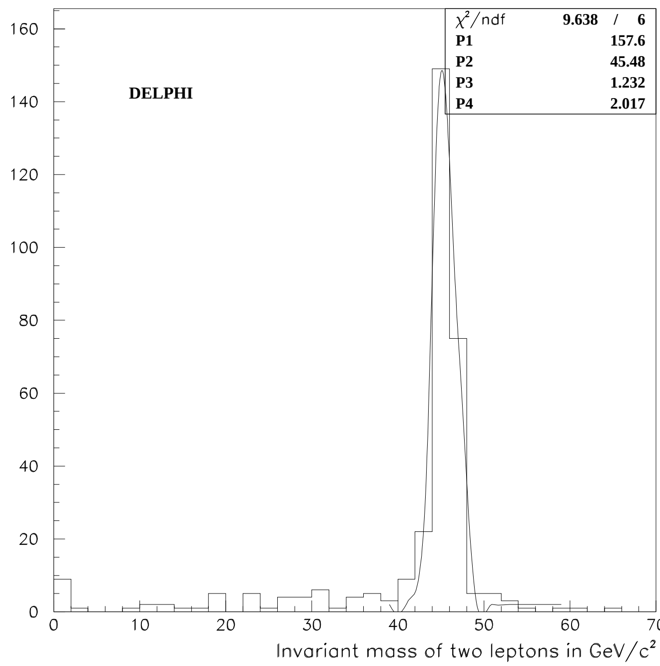

Figure 8: Invariant mass of two leptons for signal (45 GeV/c^2 sneutrino pair production) events.

Figure 8 shows the invariant mass between two leptons for the signal events before the last cut. After the cuts no event remained in the data with 0.7 expected from standard background processes. The obtained efficiency for signal events varied between 60 and 65% for sneutrinos between 45 and 70 GeV/c^2. Figure 9 shows the number of expected events as a function of the sneutrino mass. The LEP2 DELPHI data exclude a sneutrino decaying directly through the λ_{122} between 40 and 62 GeV/c^2.

Since the neutralino decays to 2 leptons and a neutrino, the indirect sneutrino decay gives finally 4 leptons and missing energy, a signature studied for the case of the neutralino. The general case will be a mixture of direct and indirect decays. By combining the direct and indirect searches, one hopes to cover the entire parameter space. By fixing the mass of sneutrino to 55 GeV/c^2 and scanning through different points of (M_2,μ) plane, the two possible decay modes (direct and indirect) of sneutrino are studied simultaneously; we combine therefore the two analyses above. The same two values of tanβ (1.5, 30) are studied. The combination of the two searches can exclude e.g a sneutrino mass of 55 GeV/c^2 at 95% C.L for all the cases apart from the deep higgsino region, i.e for low values of μ ($\mu \leq 20$) and high values of M_2($M_2 \geq$ 200). In this region, the dominant decay is $\tilde{\chi}_1^+ l^-$, and the purely leptonic decays are severely suppressed. One needs to extend the search to include the leptons + multijets signature to cover this area. Before then, no limits, independent of the chosen (indirect/direct), mode can be obtained.

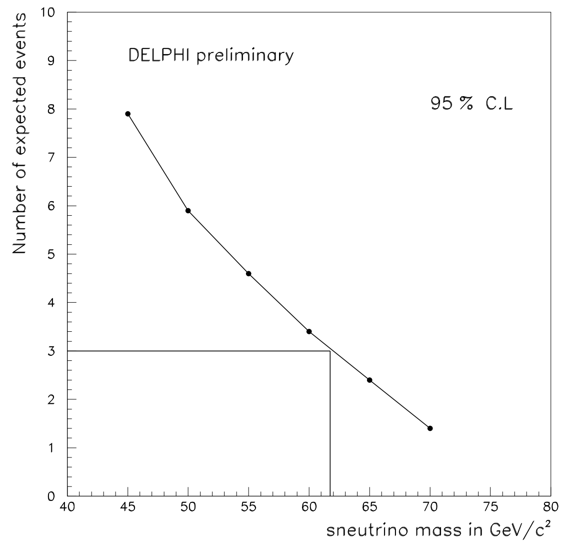

Figure 9: Expected sneutrino events decaying directly through the λ_{122} operator.

3.3 Charged slepton pair decays to 2 leptons and missing energy

When the charged slepton decays directly through the λ operator the signature is a lepton and a neutrino, giving a signature of two acoplanar leptons and missing energy. This signature is the same as the R_p decay of sleptons to the corresponding lepton and a massless neutralino, reported by DELPHI at [26]. In fact it is difficult to distinguish kinematically a neutralino of zero mass from a neutrino. One can transpose thus the limits obtained in the context of R_p studies, in the $\not{R}_p$ case, provided one assumes that the corresponding slepton is the LSP, so that indirect decays do not change the signature. Indirect decays, will in general fall in the category of multilepton studies and missing energies studied in the previous section, the combination thus of direct and indirect studies could in principle give a limit independent of the decay mode. The 95% CL lower mass limits, at $\mu \leq -200$ and $\tan\beta = 35$, obtained in [26] are 70 GeV/$c^2$for the selectrons, 58.5 GeV/$c^2$for the smuons and 52.5 GeV/$c^2$for the stau's at the limit of minimal cross section.

4 Semileptonic decays

Present experimental limits on couplings are presented in table 3.

ijk	$\lambda'_{ijk} \leq$	ijk	$\lambda'_{ijk} \leq$	ijk	$\lambda'_{ijk} \leq$
$\lambda'_{eud}/\lambda'_{\nu_e dd}(111)$	0.0004	$\lambda'_{\mu ud}/\lambda'_{\nu_\mu dd}(211)$	0.012	$\lambda'_{\tau ud}/\lambda'_{\nu_\tau dd}(311)$	0.012
$\lambda'_{eus}/\lambda'_{\nu_e ds}(112)$	0.012	$\lambda'_{\mu us}/\lambda'_{\nu_\mu ds}(212)$	0.012	$\lambda'_{\tau us}/\lambda'_{\nu_\tau ds}(312)$	0.012
$\lambda'_{ecd}/\lambda'_{\nu_e sd}(121)$	0.012	$\lambda'_{\mu cd}/\lambda'_{\nu_\mu sd}(221)$	0.012	$\lambda'_{\tau cd}/\lambda'_{\tau cd}(321)$	0.012
$\lambda'_{ecs}/\lambda'_{\nu_e ss}(122)$	0.012	$\lambda'_{\mu cs}/\lambda'_{\nu_\mu ss}(222)$	0.012	$\lambda'_{\tau cs}/\lambda'_{\nu_\tau ss}(322)$	0.012
$\lambda'_{eub}/\lambda'_{\nu_e db}(113)$	0.012	$\lambda'_{\mu ub}/\lambda'_{\nu_\mu db}(213)$	0.012	$\lambda'_{\tau ub}/\lambda'_{\nu_\tau db}(313)$	0.012
$\lambda'_{\nu_e bd}/\lambda'_{etd}(131)$	0.04	$\lambda'_{\nu_\mu bd}/\lambda'_{\mu td}(231)$	0.22	$\lambda'_{\nu_\tau bd}/\lambda'_{\tau td}(331)$	0.26
$\lambda'_{ecb}/\lambda'_{\nu_e sb}(123)$	0.012	$\lambda'_{\mu cb}/\lambda'_{\nu_\mu sb}(223)$	0.012	$\lambda'_{\tau cb}/\lambda'_{\nu_\tau sb}(323)$	0.012
$\lambda'_{ets}/\lambda'_{\nu_e bs}(132)$	0.4	$\lambda'_{\mu ts}/\lambda'_{\nu_\mu bs}(232)$	0.4	$\lambda'_{\tau ts}/\lambda'_{\nu_\tau bs}(323)$	0.012
$\lambda'_{etb}/\lambda'_{\nu_e bb}(133)$	0.001	$\lambda'_{\mu tb}/\lambda'_{\nu_\mu bb}(233)$	0.4	$\lambda'_{\tau tb}/\lambda'_{\nu_\tau bb}(333)$	0.26

Table 3: Limits on the $\not{R}_p$ couplings λ' in units of $(m_{\tilde{f}}/100GeV)$, where $m_{\tilde{f}}$ is the appropriate sfermion mass.

We searched for manifestations of the "semi-leptonic" couplings dominance in the stop pair production, where each stop decays to a lepton and a jet leading to a signature of 2 leptons and 2 jets. This is the main signature studied in this section. Indirect decays where each stop decays into charm and neutralino and subsequently the neutralino decays to a lepton and 2 jets, end up to 2 leptons and multi-jets. The effect of the indirect decay is to soften the resulting leptons. We studied only the direct decays case.

4.1 Stop decays to leptons and jets

The expression of the width of the stop decaying directly into ld (where ld can be ed, μd or e.g τb) is given by [28]:

$$\Gamma(\tilde{t}_1 \to lq) = \frac{\lambda'^2}{16\pi} cos^2\theta_t m_{\tilde{t}_1} \tag{4}$$

where θ_t is the stop mixing angle [30]. This expression may be compared to the width of the decay into $\tilde{\chi}^0_1$ which is given by [29]:

$$\Gamma(\tilde{t}_1 \to c\tilde{\chi}^o_1) = (0.3-3)\times 10^{-10} m_{\tilde{t}_1}\left[1-\frac{m^2_{\tilde{\chi}^o_1}}{m^2_{\tilde{t}_1}}\right]^2 \; GeV \tag{5}$$

The corresponding decay time ($\geq 10^{-20}$ sec) is far longer than the strong-interaction time scale of the order of 1 fm (i.e. $O(10^{-23})$ sec), so that a produced $\tilde{t}_1$ hadronizes into a stop hadron before it decays. The stop hadronization also occurs before decaying in the $\not{R}_p$ mode, for values of the λ' coupling lower than $O(10^{-1})$. As the relevant current HERA limit on λ' [6] for stop masses accessible to LEP2 already excludes λ'_{131} above $O(10^{-2})$ we will take the attitude of considering that the stop always hadronizes before decaying via $\not{R}_p$ couplings.

Equating the width $\Gamma(\tilde{t}_1 \to ld) = \Gamma(\tilde{t}_1 \to c\tilde{\chi}_1^o)$ for $\theta_t = 0$ i.e. pure left stop, gives:

$$\lambda'^2 = 16\pi(0.3 - 3) \times 10^{-10}[1 - \frac{m^2_{\tilde{\chi}_1^o}}{m^2_{\tilde{t}_1}}]^2 \tag{6}$$

So that one can estimate the accessible range of the λ' couplings involved in the direct stop decay into ld.

For conservative values in the theoretical uncertainty[29] of $\Gamma(\tilde{t}_1 \to c\tilde{\chi}_1^o)$, i.e. 3 $\times 10^{-10}$ and no suppression by phase space, one obtains the minimum value of λ', $\lambda'_{min} = 1.2 \times 10^{-4}$ above which direct decays dominate. For small mass differences between $\tilde{\chi}_1^0$ and the stop the suppression due to phase space gives a λ'_{min} closer to 10^{-5}.

For λ' below λ'_{min}, we expect that the stop decays first into charm and $\tilde{\chi}_1^0$ and then the $\tilde{\chi}_1^0$ may decay via R_p giving more complicated topologies than 2 l, 2 *jets* and no missing energy. By restricting ourselves to the 2 l, 2 *jets* and no missing energy topology, we do not explore coupling values below λ'_{min}. This very conservative value of the coupling will be taken as our limit if no evidence for this topology is found in our data.

In this section we will concentrate on the λ'_{ijk} term and more precisely on cases where:

- the λ'_{131} or λ'_{231} couplings are dominant. In this case, we have either the decay $\tilde{t}_1 \longrightarrow ed$, for the dominant coupling λ'_{131}, leading to the signature $2e$, 2 *jets* and no missing energy or the decay $\tilde{t}_1 \longrightarrow \mu d$, for the dominant coupling λ'_{231}, leading to the signature 2μ, 2 *jets* and no missing energy. The lightest stop $\tilde{t}_1$ is produced in pairs [30]. In both cases, λ'_{131} and λ'_{231}, we have the signature 2 l + 2 *jets*.
- or the λ'_{333} is dominant. There are several motivations to concentrate on this particular coupling concerning the third sfermion-fermion generation. First, there are very mild experimental constraints on λ'_{333} from the LEP I measurement of R_τ which give $\lambda'_{333} <$ 0.45 at the 2σ level or $\lambda'_{333} < 0.26$ at the 1σ level. Second, several theoretical analyses tend to indicate the possibility of having a not too small i.e. close to O(1) λ'_{333} coupling (the same for the λ'_{233} and the λ''_{233} coupling) [32] and [33]. We will therefore examine the direct decay $\tilde{t}_1 \to \tau b$ via the λ'_{333} coupling leading to the signature 2 τ and 2 b and no missing energy. We will concentrate on the topology in which the tau decays into hadrons so that the final signature we will consider is 4 jets and no substantial missing energy.

The stop and sbottom event generators used the program package GRACE [36] for the calculation of the matrix elements, and the program packages BASES and SPRING described in [35] for the phase space generation and event production. The differential cross section function is based on the calculation of [34] which includes the initial state QED correction in the collinear approximation at the leading order as well as QCD corrections. The event generator has been interfaced with JETSET 7.3 [19] in order to benefit of the facilities in treating the hadron fragmentation and decays and in order to accommodate easily the treatment required by the stop hadronization (some more details on hadronization in [30]). Numerical values for production cross sections at $\sqrt{s} = 161$ GeV and 172 GeV can be found in table 2 of [31]. We simulated stop signals at different masses and decay patterns at the two energies which then passed through DELSIM and DELANA.

4.1.1 λ'_{131} and λ'_{231} search

The selection used for the present analysis has been derived from the analysis designed for the search of the higgs boson in the hZ mode where 2 leptons (μ μ or e e) and 2 jets are produced.

This analysis has been described in [37]. The selection has only changed in some slight details and is described below.

- Hadronic events are selected by requiring at least five charged particles in the barrel acceptance and a total energy from charged particles above 12% of $\sqrt{s}$.
- Among charged particles, at least two fast charged particle with $p > 10$ GeV/c with opposite charges are required, which are then our two leptons candidates.
- Then the selection proceeds by requiring an isolation of 3^o and polar angles in the range of $[5^o, 185^o]$ for these lepton candidates, at least 2 jets in the event using a JADE-like jet algorithm and at least 2 charged particles in the second most energetic jet. Moreover, the maximum angle between the candidate lepton and the closest jet is required to be greater than 40^o while the minimum angle between the candidate lepton and the closest jet is required greater than 10^o.
- At $\sqrt{s} = 172$ GeV, additional cuts have been introduced in order to reduce further the four fermions background. Namely, *thrust* is required to be below 0.9, *sphericity* greater than 0.125 and *acolinearity* below 0.5.
- Neither lepton identification nor lepton-jet mass reconstruction have been used in the selection.

The effects of these selections in the data as well as in the simulated samples of background events are shown in table 4 at $\sqrt{s} = 161$ GeV $\sqrt{s} = 172$ GeV.

Energy	data	MC	$ff(\gamma)$	WW	ZZ	Zee	$We\nu$	$\gamma\gamma$	Bhabba
161 GeV	0	1.41 $\pm$ 0.25	0.31	0.32	0.35	0.27	0.009	0.15	0
172 GeV	1	1.08 $\pm$ 0.11	0.11	0.33	0.53	0.11	0	0	0

Table 4: Effect of the selection the for λ'_{131} and λ'_{231} search

In our selection the lepton candidates are selected with a lower momentum threshold i.e. 10 GeV, than in the case of the $h\mu\mu$ or hee analyses i.e. 15 GeV, and no lepton identification is attempted. The choice of this strategy has been imposed by the sake of optimizing the efficiencies on the signal using a single analysis designed originally for the (h,lepton lepton) channel.

4.1.2 Results

Combining Data and MC at $\sqrt{s} = 161$ GeV and $\sqrt{s} = 172$ GeV, one obtains 1 candidate in the data for 2.49 events expected in the MC. The candidate has a total energy of 169.95 GeV, a total visible mass of 169.61 GeV and missing energy of 0.73 GeV. It contains two candidate leptons of momentum 54.07 and 32.15 GeV respectively. Signal efficiencies are given in table 5.

There are no evidence for a 2 l, 2 *jets* and no missing energy topology in the data at $\sqrt{s} = 161$ GeV and $\sqrt{s} = 172$ GeV which can not be interpreted in terms of SM processes. No signal for stop decaying into ed or into μd has been found in the data. In consequence, limits on the stop mass at the 95 % confidence level, combining the results at $\sqrt{s} = 161$ GeV and $\sqrt{s} = 172$ GeV, can be derived for the ed channel and for the μd channel for two stop mixing angles corresponding respectively to the pure left stop i.e. mixing angle equal to 0, and to the stop decoupling from the Z boson i.e. mixing angle equal to 0.98 radian, denoted $\tilde{t}_{0.98}$ below.

channel	40	50	60	70	80	85
$e\ d_{161}$	31.3 ± 4.1	34.6 ± 4.5	33.1 ± 4.4	30.9 ± 4.1	24.6 ± 3.6	
$\mu\ d_{161}$	49.5 ± 5.4	34.6 ± 4.5	44.9 ± 5.0	43.3 ± 4.9	42.5 ± 4.8	
$e\ d_{172}$		18.7 ± 3.1	21.0 ± 3.3	24.2 ± 3.7	20.2 ± 3.3	16.0 ± 2.8
$\mu\ d_{172}$		32.4 ± 4.1	31.4 ± 3.9	33.4 ± 4.1	29.4 ± 3.7	27.0 ± 3.5

Table 5: Signal efficiencies (in %) for the λ'_{131} and λ'_{231} search

The two stop decay channels have to be considered separately since we are considering two different $\not{R}_p$ couplings.

The results are shown in table 6.

$\tilde{t}_1 \rightarrow ed$	$\tilde{t}_1 \rightarrow \mu d$
$m_{\tilde{t}_L} > 66.93$ GeV 95 % C.L.	$m_{\tilde{t}_L} > 69.51$ GeV 95 % C.L.
$m_{\tilde{t}_{0.98}} > 50.03$ GeV 95 % C.L.	$m_{\tilde{t}_{0.98}} > 58.69$ GeV 95 % C.L.

Table 6: Stop mass limits

In the case of a zero stop mixing angle i.e. a pure left stop, λ'_{min} has been established conservatively to be equal to 1.1 10^{-4}, so that we have the boundaries λ'_{131} and $\lambda'_{231} < 1.1\ 10^{-4}$. In the case of a mixing angle equal to 0.98 i.e. stop decoupling from the Z boson, the above value of the couplings have to divided by $cos(0.98) = 0.557$ (see equation 4) which gives 1.9 10^{-4} for λ'_{131} and λ'_{231} respectively. In the case of a pure left stop the exclusion domain in the λ'_{131} and $m_{\tilde{t}_1}$ plane are shown in figure 21 and compared with other searches from DELPHI, LEP and HERA. While the range of accessible stop masses is modest when compared to the range of H1, λ'_{131} coupling values can be excluded down to the 10^{-5} level which are about 2 orders of magnitude below the H1 limits. Even lower coupling values can be explored when considering more complicated signatures than 2 l, 2 $jets$ and no missing energy i.e. signature in which the stop first goes into charm and $\tilde{\chi}^0_1$ and then the $\tilde{\chi}^0_1$ decaying via the λ'_{131} $\not{R}_p$ coupling. Such topologies will be studied in a future work.

4.1.3 λ'_{333} search

The selection used for the present analysis has been derived from the analysis designed for the search of the higgs boson in the hZ and hA mode where 2 τ and 2 jets are produced. This analysis has been described in [37]. The selection has only changed in some slight details for the last three cuts. One concerns the b-tagging which has been tightened so that the b-tagging variable P_E^+, which is the event probability computed from tracks with positive impact parameters only, is now required to be below 10^{-3}. The two other cuts concern the $m_{\tau\tau}$ and $m_{jet\,jet}$ masses which have been removed and replaced by a cut on τb pair mass differences in those combination for which the mass difference of the two possible τb pairing is minimum. We require that this mass difference is lower than 40 GeV. The result of this selection on signal efficiencies can be seen in table 7.

$m_{\tilde{t}_1}$ in GeV	50	60	70	80
$\sqrt{s} = 161$ GeV	12.2 $\pm$2.1	15.8 $\pm$2.2	18.8 $\pm$1.8	23.6 $\pm$2.6
$\sqrt{s} = 172$ GeV	12.9 $\pm$1.7	13.0 $\pm$1.7	14.3 $\pm$3.3	24.0 $\pm$1.6

Table 7: Signal efficiencies (in %) for the λ'_{333} search

4.1.4 Results

No candidate is found in the data while we expect 0.225 ± 0.050 from processes from the Standard Model simulated by MC. In consequence, limits on the stop mass at the 95 % confidence level, combining the results at $\sqrt{s} = 161$ GeV and $\sqrt{s} = 172$ GeV, can be derived for the τd channel for two stop mixing angle corresponding respectively to the pure left stop i.e. mixing angle equal to 0, and to the stop decoupling from the Z boson i.e. mixing angle equal to 0.98 radian.

We exclude a $m_{\tilde{t}_L} > 59.3$ GeV/c^2 at 95 % Confidence Level. In the case of a pure left stop, for the reasons that have been explicited above, we have the boundary $\lambda'_{333} < 1.1\ 10^{-4}$.

5 Hadronic decays

The existing constraints on λ''_{ijk} couplings are shown in table 8. These are limits on operators.We choose to disregard limits on products of operators, given our hypothesis of a single operator dominance.

ijk	$\lambda''_{ijk} \leq$	ijk	$\lambda''_{ijk} \leq$	ijk	$\lambda''_{ijk} \leq$
$\lambda''_{usd}(121)$	10^{-6}	$\lambda''_{csd}(221)$	1.25	$\lambda''_{tsd}(321)$	0.97
$\lambda''_{ubd}(131)$	10^{-4}	$\lambda''_{cbd}(231)$	1.25	$\lambda''_{tbd}(331)$	0.97
$\lambda''_{ubs}(132)$	1.25	$\lambda''_{cbs}(232)$	1.25	$\lambda''_{tbs}(332)$	0.97

Table 8: Limits on the $\not R_p$ couplings λ'' in units of $(m_{\tilde f}/100GeV\ )$, where $m_{\tilde f}$ is the appropriate sfermion mass.

In this section we will treat the hadronic multijet events coming from the decay through the operators λ''_{ijk} and λ'_{ijk}. There will be 3 types of events in these topologies.

- Chargino and neutralino decays to multijet (more than 4 jets) topologies through the operators corresponding to λ''_{ijk}. The arguments concerning the neutralino having a smaller mass than the chargino have been developed in section 3. We can safely assume that the lowest mass neutralino will decay directly to 3 jets ($\tilde\chi^0_1 \rightarrow \bar u \bar d \bar d$). Its pair production will give a 6 jet topology. We search for peaks in a 6 jet topology. On the other hand the indirect decay of the chargino to the neutralino plus an off-shell W is dominant in practically all the phase space, apart from cases of extreme degeneracy of the chargino and the neutralino. In these special cases the chargino decays directly and the first analysis can be transposed without any change. In the rest of the parameter space it decays indirectly giving a final 10 jet topology.
- Squark decays to 4 jet topologies through the operator corresponding to λ''_{ijk}. Among the squarks the third generation has the highest probability to be the first accessible to a e^+e^- collider due to mixing and the strongest influence of Yukawa couplings. The stop would decay to 2 down quarks ($\tilde t \rightarrow dd$) and the sbottom to an up and a down quark ($\tilde b \rightarrow ud$). For the case of the light stop where the $\not R_p$ decays are going through C.K.M suppressed matrix elements, the direct decay dominates for a large region of values of λ''. On the contrary the decay of a sbottom to a b and $\tilde\chi^0_1$ dominates whenever it is kinematically possible giving 8 jet topologies.
- Charged slepton and sneutrino decays to 4 jet topologies through the operator corresponding to λ'_{ijk}. The charged sleptons decay to an up and down quark, while the sneutrinos decay to two down quarks. Table 3 shows charged sleptons can decay through 6 couplings with $2b$'s in the products, 12 couplings without b's and 9 couplings are inaccessible; while the sneutrino decays through 15 couplings with b's in the products and 12 without. The direct decay is comparable to the indirect for high λ' values even when the neutralino mass is quite far from the parent sfermion, so a direct decay search for 4 jets is particularly sensitive. The indirect decays give a charged lepton or a neutrino and a neutralino which in turn decays to a lepton and 2 jets. So mixed events consisting of leptons missing energy and jets are produced. These topologies will be studied in a later publication. We will take the third generation cross-section, conservatively avoiding thus the region where

the first generation cross-section is enhanced due to exchanges in the t channel. Therefore the case where the stau is the LSP will be covered.

5.1 Chargino and neutralino decays to more than 4 jets

The particularity of these channels comes from the necessity to go beyond the common 4-jet event analysis. In the case of the neutralino or a chargino decaying directly we search for two heavy objects with the same mass which decay in 3 quarks. A clusterization of the particles in 6 jets has to be performed in order to estimate the energy and direction of the initial partons. The main backgrounds come from QCD events (e.g. $Z\gamma \longrightarrow q\bar{q}\gamma$ with gluon emission) and from the W pair 4-jet events.

Due to the backgrounds, the selection of the 6-jet signal requires a multi-jet analysis. In our analysis each event is clusterized in 2 to 6 jets. The 2- 3- 4- and 5-jet topologies are used to cut the QCD and WW events, while the 6-jet topology is used to reconstruct the masses of the two objects.

This task is performed by using the Durham clustering algorithm [38] which gives for each event the different possible clusterizations from 2 to 6 jets, with corresponding values of the y_{min} distances between the two closest jets [e.g. $y_{min}(ij) = 2min(E_i, E_j)(1 - \cos\theta_{ij})$]. For example, y_{34} is the value of y_{min} for which the event goes to from a 4-jet to a 3-jet topology and can be used to select 4-jet events.

After QCD, WW and ZZ cuts, we performed for the six jets configuration a multi-jet rescaling [39] imposing conservation of energy and momentum.

In order to reconstruct the two masses we must choose one combination of three jet pairs among 10 possible combinations. Selection criteria are imposed on the maximum θ^{ij}_{max} and the minimum θ^{ij}_{min} angles between each jet of the same object. A combination of 3 jets with $\theta^{ij}_{min} \geq 90$ degrees and $\theta^{ij}_{max} \geq 160$ degrees is rejected. These selection optimize the resolution for heavy object with a mass between 30 and 70 GeV. Then we choose the combination which has the lower value of $\mid Ma - Mb \mid \; + \; \mid Ea - Eb \mid$ and which has a difference of mass $\mid Ma - Mb \mid$ lower than 10 GeV (a and b stands for a and b reconstructed 3-jet objects).

With the prescription given above we can reconstruct a signal of two neutralinos from $m_{\tilde{\chi}^0_1} = 45$ GeV/c^2 to 60 GeV/c^2 with a resolution of 4 GeV/c^2 for the sum of the 2 masses and 50% efficiency. The 50% on-peak reconstruction efficiency is a major advantage of this algorithm given the complexity of these 6-jet events.

5.1.1 $\lambda''_{usd}(221)$ search

The selection of the 6 jets signal is performed in 4 steps :

- Standard hadronic selection and anti-ISR cuts
  - Hadronic selection : Charged particles $\geq$ 12, $E_{charged} \geq 0.30\sqrt{s}$, $E_{total} \geq 0.12\sqrt{s}$ and $E_{eem} \leq 0.70\sqrt{s}$
  - Anti-ISR cuts in 2-jet topology : the energy E^{cal}_{γ} of radiative γ lost in the beam pipe is calculated using energies and directions of the 2 jets coming from the Z. Events with $E^{cal}_{\gamma} \geq 25$ GeV are rejected.
  - Anti-ISR cuts in 3-jet topology : The electromagnetic energy of the jet must be lower than $0.9 \times E^{jet}$ and the number of charged particles of the jet must be greater or equal to 2. These criteria cut events with the ISR photon in one of the jet.

- We cut also events with detected γ at $E_\gamma^{mes} \geq 25$ GeV and with undetected γ (lost in the beam pipe) requiring a $P^{miss} \leq 35$ GeV.

- Anti-QCD cuts
  - Selection in 4-jet topology : following standard hA and hZ 4-jets analysis we cut the QCD background with gluon emission along the quarks with the following function [41] : $\alpha_{min}\ E_{min}\ \geq\ 19.5\ -\ 4.5\ \beta_{min}\ \frac{E_{max}}{E_{min}}$ where α_{min} means the minimum angle between the 4 jets, β_{min} means the minimum angle between the highest energetic jet and the three others and E_{max} (E_{min}) are the maximum (minimum)jet energy. We also require $\alpha_{min}\ E_{min}\ \geq\ 5$ GeV and $\beta_{min}\frac{E_{max}}{E_{min}} \geq\ 1$.

- Anti-WW cuts
  - Selection in 4-jet topology is performed with a standard 4 jets 5C fit requiring equal masses. If the mass m^{fit5C} is greater than 72 GeV with a normalised $\chi^2 \leq 2$, the event is considered as a WW event and it is rejected.

- 6-jet selection
  - In order to have a least five good separated jets we cut on the Durham distance y_{45} at 0.0015
  - We require a difference of rescaled masses $\mid M_a - M_b \mid \leq 10$ GeV.

The effect of these cuts on the real data and on the simulated backgrounds is given in table 9. Real data and simulated standard model events are in a good agreement.

This can be seen in the final result obtained for the sum of masses represented in Figure 10.

cut	observed events	expected SM events	QCD	WW	ZZ
Hadronic preselection with anti-ISR	602	580.2	482.5	71.2	26.5
anti-QCD	196	199.9	124.0	59.2	16.7
anti-WW	166	163.7	116.6	31.7	15.4
6 jets	34	34.9	18.1	13.8	3.0

Table 9: Number of events remaining after each cut on the data and the simulated normalized background.

The efficiency for the signal after the cuts, in a 2 σ window around each reference mass is 25% for masses from 45 to 60 GeV/c^2. Since no obvious peak is seen we scan the mass plot in a window of $\pm$ 2 σ and extract a limit for each mass. We exclude therefore for these masses a neutralino or chargino directly decaying into 3 jets, with a cross section of 1.4 pb at 95% CL.

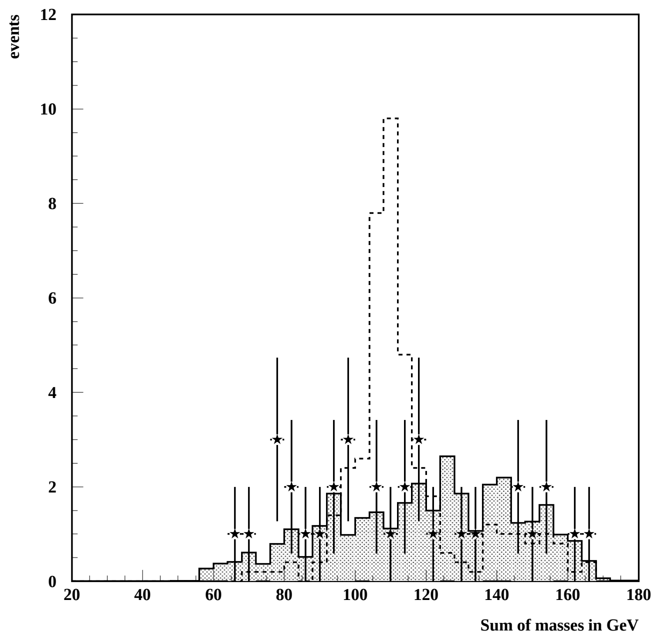

Figure 10: Sum of the two 3-jet masses after all cuts, in multijet search, compared to normalized background and a 6 jet signal.

5.2 Stop and sbottom decays to 4 jets

The λ''_{332} and λ''_{323} R-parity violating terms correspond to the stop decay to sb quarks giving rise to a 4 jets with no missing energy topology. The selection used for this 4 jets topology search has been taken from the search for hA into 4 b jets described in [37]. With this selection, no candidates were found in the DATA at $\sqrt{s}$ = 161 GeV and $\sqrt{s}$ = 172 GeV while 1.8 ± 0.2 events were expected from the MC simulation of the processes of the Standard Model. The result of this selection on the $\tilde{t} \to sb$ signal in terms of efficiencies can be seen in table 10. No signal for

$m_{\tilde{t}_1}$ in GeV	50	60	70	80
$\sqrt{s}$ = 161 GeV	16.1 ± 2.6	18.6 ± 2.8	19.6 ± 2.8	14.6 ± 2.5
$\sqrt{s}$ = 172 GeV	11.6 ± 2.3	12.6 ± 2.3	15.1 ± 2.5	15.1 ± 1.8

Table 10: Signal efficiencies.

stop decaying into sb has been found in the data. In consequence, limits on the stop mass at the 95 % confidence level, combining the results at $\sqrt{s}$ = 161 GeV and $\sqrt{s}$ = 172 GeV, can be derived for the sb channel. For a stop mixing angle $\theta_t = 0$, we have $m_{\tilde{t}_1} > 61.0$ GeV/c^2 at 95 % Confidence Level. In the case of a zero stop mixing angle, a value λ''_{min} can be established conservatively 1.1 10^{-4}, so that we have the limits $\lambda''_{323} < 1.1\ 10^{-4}$ and $\lambda''_{332} < 1.1\ 10^{-4}$.

5.3 Stau and sneutrino pair decay to 4 jets

The sneutrino decays to $d\bar{d}$ through the $\not{R}_p$ term $\lambda'_{\nu_\tau dd}(311)$ and to $d\bar{b}$ or to $b\bar{b}$ quarks through the $\lambda'_{\nu_\tau db}(313)$ and the $\lambda'_{\nu_\tau bb}(333)$ terms respectively.

Hadronic events are selected by requiring at least 12 charged particles, a total of charged energy above $0.30\sqrt{s}$ and a total energy exceeding $0.40\sqrt{s}$. In order to reduce the radiative $q\bar{q}\gamma$ background a cut on the maximum photon energy E_γ^{max} or E_γ^{cal} to be less than 35 GeV is applied.

The DURHAM algorithm [38] is used to reconstruct a four jet event. A y_{cut} value of 0.003 is applied. If the number of jets is less than four then the event is rejected otherwise it is forced by to be a four jet event.

5.4 The $\lambda'_{\nu_\tau dd}(311)$, $\lambda'_{\nu_\tau db}(313)$, $\lambda'_{\nu_\tau bb}(333)$ search.

The same selection criteria are applied for all the λ'_{3jk} terms while b tagging is applied only for the $\lambda'_{\nu_\tau db}(313)$ and $\lambda'_{\nu_\tau bb}(333)$ searches. The selection criteria are the following:

- All four jet events are required to satisfy energy and momentum conservation by applying a kinematical(4C) fit [40]. Then the χ^2_{4C} is required to be less than 25 to reduce the badly reconstructed or radiative events.
- The remaining radiative $q\bar{q}\gamma$ background can be further reduced by requiring a jet to have at least 2 charged particles, an electromagnetic energy less than $0.8E_{jet}$ and a mass m_{jet} greater than 1 GeV/c^2.
- The QCD background is further reduced by applying a cut on the following four jet event shape variables [41]: The product $\alpha_{min} \times E_{min}$, where α_{min} is the minimum angle between two jets and E_{min} the lowest energy of the jets and $\beta_{min} \times \frac{E_{max}}{E_{min}}$, where β_{min} is the minimum angle between the highest energetic jet and the three others. The $\alpha_{min} \times E_{min}$ is required to be greater than $15 + 0.5 \times \beta_{min} \times \frac{E_{max}}{E_{min}}$.
- The 4-parton matrix element for $e^+e^- \to q\bar{q}gg$ is calculated as defined in [42]. A "QCD-probability" P_{QCD} is formed, taking as inputs the jet four vectors, and only events with low P_{QCD} are retained.
- The mass reconstruction is done by applying a kinematical fit with five constraints(5C) [40], where the additional fifth constraint requires the production of two equal mass objects. For a 45 GeV/c^2sneutrino a resolution of 1.42 GeV/$c^2$is obtained.

The event and jet tagging is using the AABTAG algorithm [43]. This algorithm combines information from impact parameters and rapidities of the tracks, the masses from the secondary vertices and the fraction of the energy taken by B-hadrons in the jets. An event tagging variable T_{4b} [43] is defined to distinguish four b-jet events from QCD and WW event topologies. The distributions of the event probability for positive impact parameters $-log_{10}(prob^+)$ and the tagging variable T_{4b} are given in figure 11.

For the $\lambda'_{\nu_\tau db}(313)$ search (2b's in the event) the $prob^+ < 10^{-1}$ is required, while for the $\lambda'_{\nu_\tau bb}(333)$ search (4b's in the event) the additional requirement $T_{4b} >$ -2 is applied.

Results are summarized in table 11. Full agreement between DATA and MC is found for the all the $\not{R}_p$ terms. The distributions of DATA and SM background processes before b-tagging is shown in figure 12. One candidate with mass equal to 41.7 GeV/$c^2$is left after b-tagging is applied while 0.6 are expected from the SM background at 171 GeV.

Selection criteria	DATA	$q\bar{q}\gamma$	W^+W^-, Z^0Z^0	eff.(%), $\lambda'_{\nu_\tau db}(313)$ $m_{\tilde{\nu}_\tau} = 45$ GeV$/c^2$
Four jets, $y^D_{cut} > 0.003$	87(110)	75.9(52.2)	16.44(63.1)	66
$\chi^2_{4C} < 25$	72(95)	63.7(45.3)	14.68(56.9)	62
ISR and QCD	15(38)	9.2(9.3)	10.35(39.3)	35
$prob^+ < 10^{-1}(\lambda'_{\nu_\tau db}(313))$	4(13)	3.1(2.8)	2.8(9.9)	32
$T_{4b} > -2(\lambda'_{\nu_\tau bb}(333))$	0(1)	0.7(0.4)	0.05(0.2)	

Table 11: DATA, SM background events the signal efficiency for a $\tilde{\nu}_\tau$(produced at 172 GeV) with mass equal to 45 GeV$/c^2$at center of mass energy of 161 (172) GeV.

For the $\not{R}_p$ terms $\lambda'_{\nu_\tau dd}(311)$, $\lambda'_{\nu_\tau db}(313)$ and $\lambda'_{\nu_\tau bb}(333)$ the efficiencies for different sneutrino masses are presented in table 12. In the latter two terms the b-tagging algorithm is applied.

$\not{R}_p$ terms	45 GeV$/c^2$ eff.(%)	50 GeV$/c^2$ eff.(%)	55 GeV$/c^2$ eff.(%)	60 GeV$/c^2$ eff.(%)	65 GeV$/c^2$ eff.(%)
$\lambda'_{\nu_\tau dd}(311)$	33(32)	43(41)	45(47)	48(50)	49(53)
$\lambda'_{\nu_\tau db}(313)$	30(28)	38(36)	43(42)	44(44)	47(48)
$\lambda'_{\nu_\tau bb}(333)$	30(30)	40(39)	44(45)	48(48)	51(49)

Table 12: The efficiency as a function of the $\tilde{\nu}_\tau$ mass after all cuts at center of mass energy of 161 (172) GeV.

5.4.1 Results

A preliminary limit at 95% confidence level is calculated for the $\lambda'_{\nu_\tau bb}(333)$ violating term where there is no candidate above 45 GeV$/c^2$. The number of expected events as a function of mass at the center of mass energy of 161 and 172 GeV respectively is plotted in figure 13. At 95% confidence level masses lower than 57.5 GeV$/c^2$are excluded.

For the other $\not{R}_p$ terms the sensitivity of a single experiment, given the available luminosity is not sufficient to give robust limits. Nevertheless, a preliminary limit is obtained for the $\lambda'_{\nu_\tau db}(313)$ violating term. At 90% confidence level sneutrino masses lower than 56.8 GeV$/c^2$ are excluded. Finally for the $\lambda'_{\nu_\tau dd}(311)$ term the luminosity available is not sufficient to obtain a 90 % CL limit. A combination of the results of at least three experiments, or the assumption that the 3 operators $\lambda'_{\nu_\tau dd}(311)$, $\lambda'_{\nu_\mu dd}(211)$ and $\lambda'_{\nu_e dd}(111)$ are different from zero, profiting from the extra production of $\tilde{\nu}_\mu$ and $\tilde{\nu}_e$, at the same mass.

The analysis for the sneutrino is also applied to stau $\not{R}_p$ term $\lambda'_{\tau ud}(311)$. The analysis and the efficiencies of detection are the same as these of $\lambda'_{\nu_\tau dd}(311)$ search . The result is shown in figure 13. For the production cross section a left $\tilde{\tau}$ has been assumed. Here too more luminosity or a combination of results is needed.

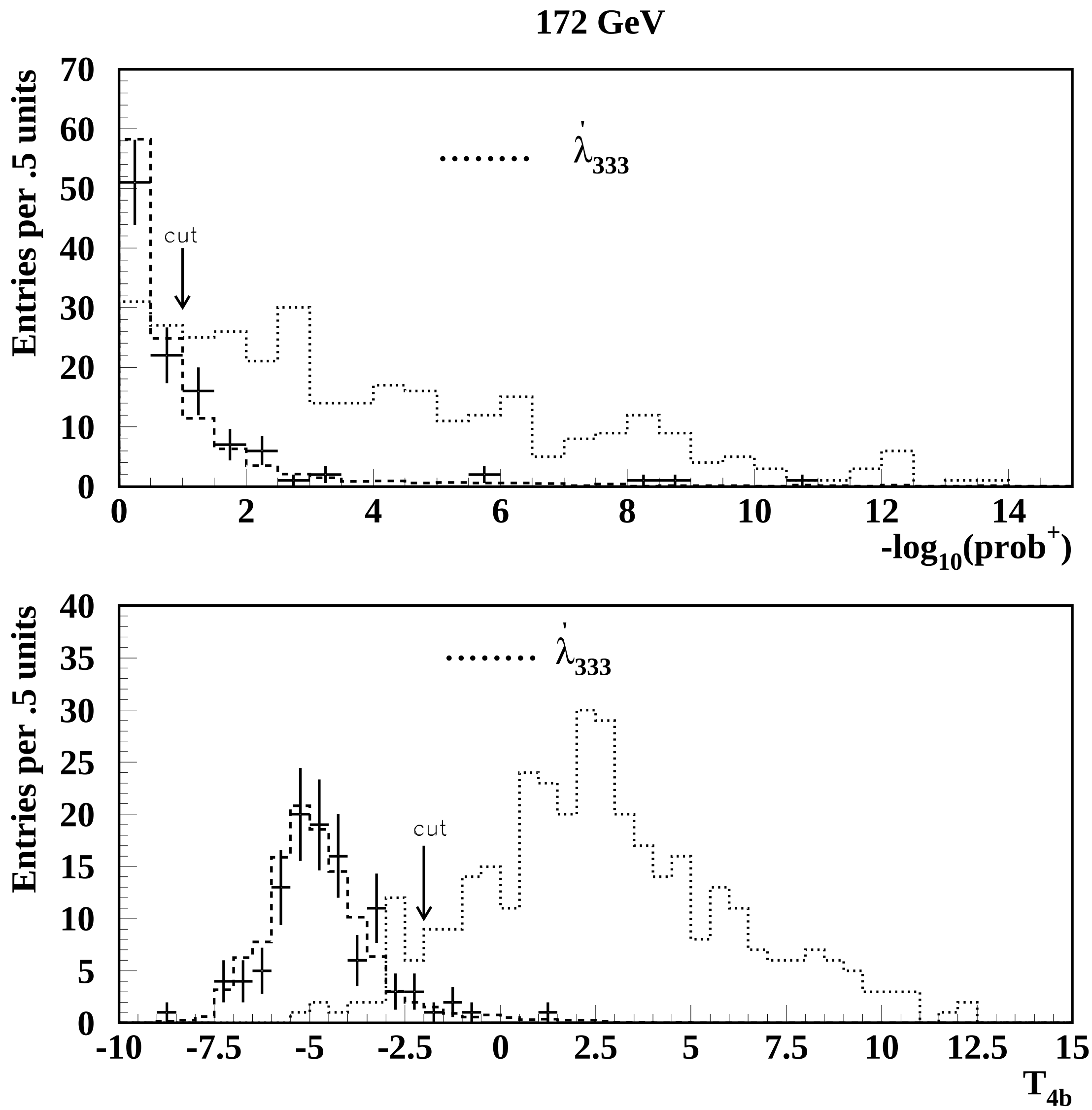

Figure 11: Distributions of b tagging variables after the four jet selection. DATA(plotted with statistical error bars), SM(QCD, $W^+W^-$and Z^0Z^0 background plotted with hatched line) and a $\tilde{\nu}_\tau$ with mass equal to 45 GeV/c^2(plotted with dotted line and arbitrary normalization).

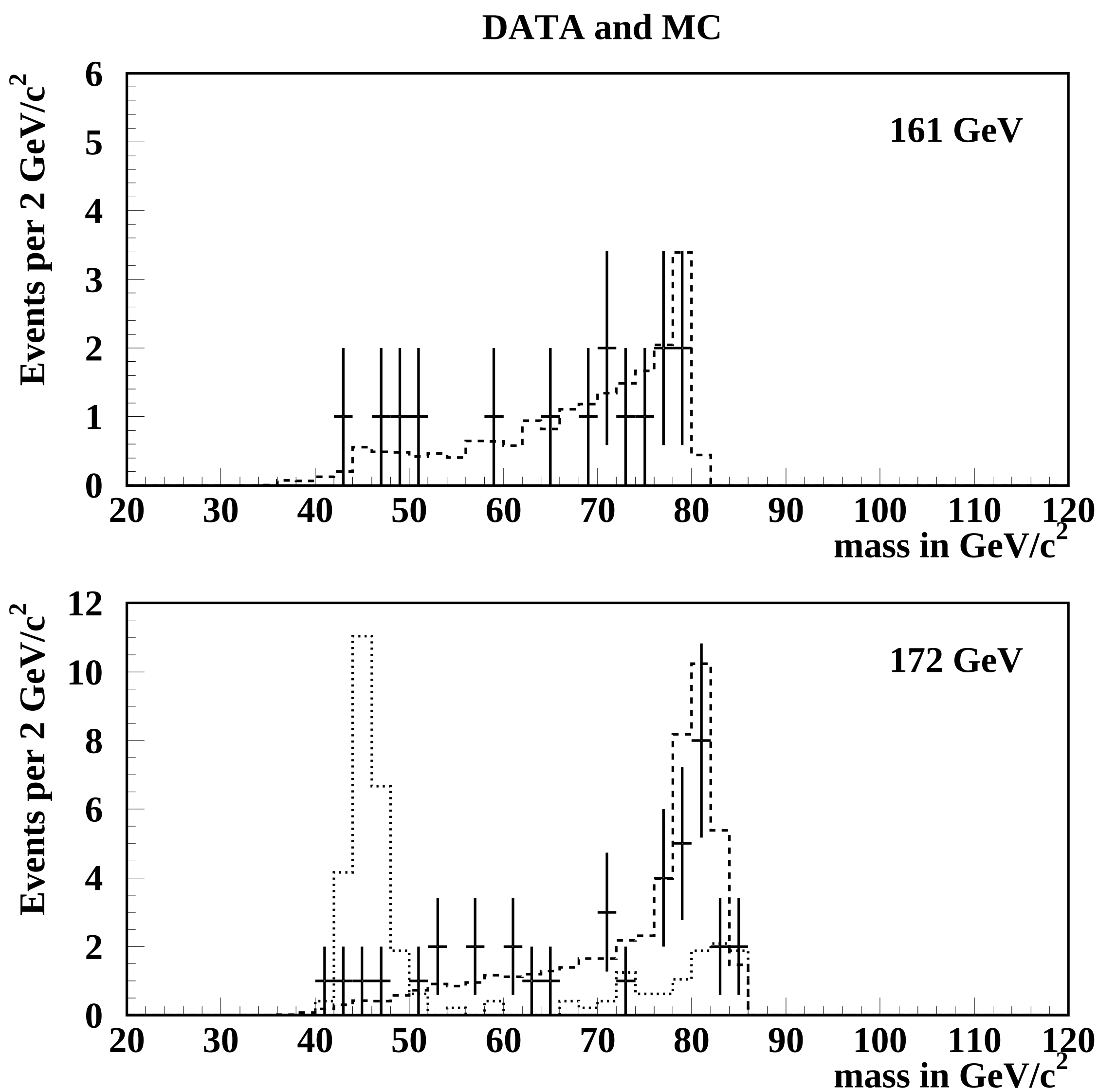

Figure 12: DATA(plotted with statistical error bars), SM(QCD, $W^+W^-$and Z^0Z^0 background plotted with hatched line) and a $\tilde{\nu}_\tau$ with mass equal to 45 GeV/c^2(plotted with dotted line and arbitrary normalization) before b-tagging is applied.

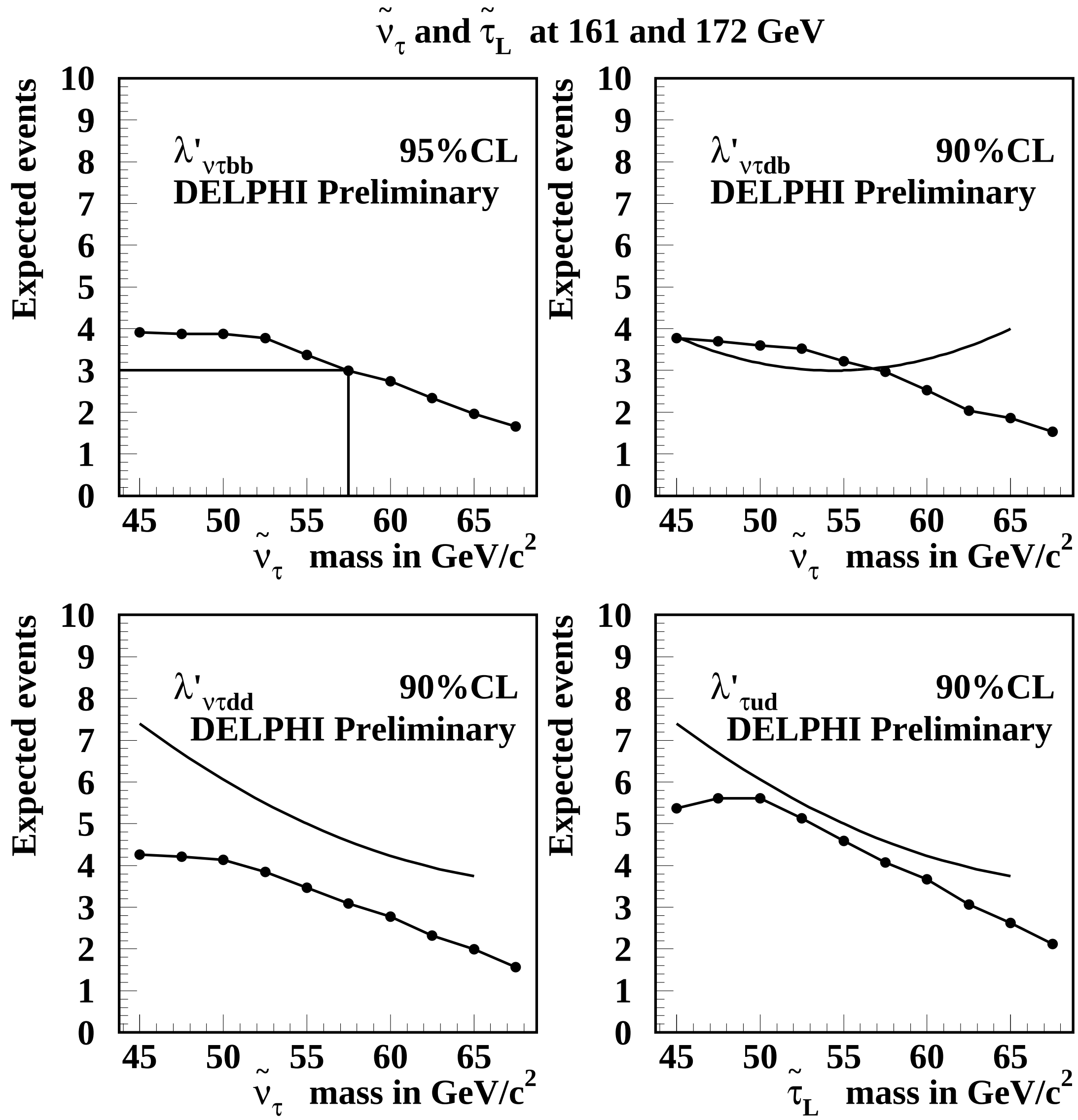

Figure 13: Expected events (dots connencted with a solid line) versus mass at 95% and 90% CL for the $\lambda'_{\nu_\tau dd}(311)$, $\lambda'_{\nu_\tau bb}(313)$, $\lambda'_{\nu_\tau bb}(333)$ and $\lambda'_{\tau ud}(311)$ terms.

6 Single sparticle production

6.1 Single squark production

The analysis of [44] covers the search for leptoquarks produced singly, decaying through the charged mode at center-of-mass energies of $\sqrt{s} = 161$ GeV and $\sqrt{s} = 172$ GeV. Since the signal of a direct decay of a squark, is the same as the one of a scalar leptoquark, we will transpose the searches of this paper, in a $\not{R}_p$ supersymmetric context. The main difference, is the fact that a squark will have a mixture of R_p and $\not{R}_p$ decays. A complete scan of the supersymmetric parameter space is beyond the scope of this paper, so we will assume that the searched squarks are the LSP's having only $\not{R}_p$ modes.

The highest contribution to the total cross section, comes from the resolved photon contribution [45], where the hadronic contents of a Weizacker-Williams photon radiating off from one of the initial electrons is taken into account. The GRV parameterization [46] of the parton distribution is used. Since the photon has different u-quark and d-quark contents, the production of the corresponding squarks will also be different. On the other hand, the production cross section being basically proportional to $(1+q)^2$ the squarks of charge q=-1/3 (-2/3) will be produced with different production cross sections.

Charged decays of singly produced high mass squarks would be characterized by a high transverse momentum jet recoiling against an electron. Some hadronic activity can be present in the forward region, originated from the remanent of the quasi real photon. The initial electron which scatters the quasi real photon was assumed to escape detection. Thus, final state topologies would be energetic mono-jet topologies with one well isolated energetic electron and eventually a low energy jet in the forward region of the detector.

Events were considered to have a mono-jet topology if the Durham resolution variable (y_{cut}) in the transition from two to one jet was lower than 0.09. Events were considered to have a two-jet topology if the resolution variable y_{cut} associated to the transition from three to two jets was lower than 0.03.

In a very loose identification, charged tracks were considered to be isolated energetic electrons if their momenta were higher than 10 GeV/c, if there were no associated hits in the muon chambers, and if in the double cone centered on each track with internal and external half-angles of 5° and 25° the charged energy and the neutral energy were less than 1 GeV and 2 GeV respectively. Inside the inner cone no other charged track was allowed. Due to the very low background no requirement on the associated electromagnetic energy was made.

To the obtained sample of events with one or two jets and one isolated electron, the following selection criteria were applied:

- the electron and jets had to be between 30° and 150° in polar angle,
- the most energetic jet should be $>$ 10 GeV and the less energetic $<$ 30 GeV,
- the angle between the lepton and the most energetic jet had to be larger than 90^0.

In order to reduce the contamination from semileptonic decays of WW pairs, an additional cut was applied rejecting events with both the missing transverse momentum and the momentum of the electron inside a window of ± 10 GeV around 40 GeV.

One and two events were found in the data at $\sqrt{s}$ =161 GeV and $\sqrt{s}$ =172 GeV, respectively. The expected SM background is 2.4 ± 0.5 at $\sqrt{s}$ =161 GeV and 1.8 ± 0.5 $\sqrt{s}$ =172 GeV.

The jet-lepton invariant mass distribution shows no evident clusterizations and it is in agreement with the MC expectation. Within the low statistics there is a reasonable agreement between data and SM predictions. The mass resolution at 100 GeV/c^2 is 12 GeV/c^2. The efficiency was found to be between 30% and 56% for squark masses in the range from 80 GeV/c^2 up to the kinematic limit for both $\sqrt{s} = 172$ GeV and $\sqrt{s} = 161$ GeV.

The limits obtained can be interpreted in terms of the squark coupling parameter λ'. Limits on λ' as a function of the squark mass are shown in figure 21 for both up and down squarks.

6.2 $\tilde{\nu}$ resonant production

The most spectacular manifestation of $\not{R}_p$ could be the presence of a sneutrino resonance. This reaction arises from a s-neutrino resonant production via the couplings λ_{121} and λ_{131}. With initial state radiation, there is an excellent sensitivity for masses below the center of mass energy.

6.2.1 $\tilde{\nu} \rightarrow \tilde{\chi}^0_1 \nu$

Since no significant deviation has been observed at LEP2 for the leptonic channels, one may assume that λ has to be smaller than the standard coupling constant and it seems therefore natural to assume that the produced sneutrino could decay into an R-parity allowed mode. If this mode has some missing energy features - e.g. $\tilde{\nu} \rightarrow \chi\nu$ with $\chi \rightarrow e^+e^-\nu$ - DELPHI searches give a high sensitivity to this type of mechanism. In the example given above, the signal can be observed in the DELPHI selectron search [26] with a large efficiency (40-60 %) and with low background (1 candidate for 161+172 GeV data). One can therefore derive upper limits on λ at the few 10^{-3} level in the mass range below 172 GeV (figure 14).

6.2.2 $\tilde{\nu} \rightarrow l_i^{\pm}\chi^{\pm}$

On the other hand, a dedicated search for signals from the sneutrino resonance R_p decay mode producing a single chargino production has been performed under the assumption that the dominant $\not{R}_p$ couplings involve only leptonic fields ($\tilde{\nu} \rightarrow l_i^{\pm}\chi^{\pm}$). where $i = 2$ or 3 for a charged lepton of the second or third family. The goal of this study was to determine the minimum $\not{R}_p$ coupling that can be probed when the energy at the center of mass is *on the resonance*.

The produced chargino decays either directly, via the R-parity violating coupling, or via cascade decay, depending on the $\chi_1^{\pm}$ and χ_1^0 mass difference and the λ Coupling. The most interesting final topology involves 4 leptons with or without missing energy, a signature similar to the one studied in section 3.

A dedicated analysis has been performed for the final state of four charged leptons with or without missing energy. Events have been selected if they satisfied the following criteria:

- The multiplicity of the event to be bigger than 3 and smaller than 10;
- The energy measured by the STIC Calorimeter to be below 15 GeV;
- The total energy to be greater than 40 GeV and the visible energy greater than 30 GeV. The energy carried by the neutral particles was required to be less than 20 GeV;
- Four charged particles with momentum above 5 GeV and with $20^o < \theta < 160^o$. The charge sum was equal to zero;
- At least two identified leptons with one identified loose muon;

Cuts	data events 161 GeV	Expected SM events 161 GeV	data events 172 GeV	Expected SM events 172 GeV
$4 \leq N_{total} < 10$ $E_{STIC} < 15GeV/c^2$	612	590.	584	570
$E_{charged} \geq 30GeV$ $E_{neutral} < 20GeV$	349	330.	341	320.
$N_{charged} = 4$ $2\ leptons, (1\ Muon)$	3	2.1	4	3.
$\Theta^{min}_{lepton-track} \geq 10^o$	0	0.3	2	0.6
$M_{ll} > 2.GeV/c^2$	0	0.2	1	0.3

Table 13: Number of events remaining after each cut on the data and the simulated normalized background.

- Each charged track was isolated without other charged tracks around inside a cone of 10 degrees;
- The invariant mass of every two charged tracks to be greater than 2 GeV/c^2

The Standard Model background was estimated using simulated samples from four-fermion final states , especially $2e$ 2μ , $Z\gamma$, $\gamma\gamma$,WW and Bhabha events. The SM background for exotic events with lepton number violation is zero. Effect of the cuts on real data and on the simulated background are given in Table 13 for the center of mass energies of 161 and 172 GeV.

The efficiencies are dependent on the parameters of the MSSM model chosen for the simulation. Table 14 contains the results from efficiency calculation of fully simulated events for three points of the MSSM parameter space. The Table also contains the mass of the singly produced $\chi_1^{\pm}$ and the corresponding model-independent cross-section upper limits at 95 % C.L.

An upper limit 0.003 is given on the λ_{121} coupling at 95 % confidence level for the s-neutrino resonant production via the coupling λ_{121}.

Although a complete study of these limits requires a scanning of the MSSM parameter space, these first results from the search of Single Chargino production probe a mass region naturaly well above the limits obtained for pair chargino production.

6.2.3 $\tilde{\nu} \to b\bar{b}$

If both R-parity violating mechanisms (λ and λ') are present, $\tilde{\nu}$ can decay into d$\bar{d}$ and one could observe an excess in down quark channels (note that, due to helicity conservation, this diagram does not interfere with the SM terms). Assuming, as in [32], that the largest coupling is to b$\bar{b}$, a specific study has been performed. Figure 15 shows the mass distributions observed by DELPHI for b$\bar{b}$ final states. Data are peaking at nominal $\sqrt{s}$ with large tails due to initial state radiation. No obvious structure is observed within these tails. Figure 14 gives the corresponding limit on λ. This limit is obtained by optimizing the mass integration range given the predicted background with the assumption that the total width is of the order of 8 GeV (as given in [32]). Since limits are similar in both scenarios, one may argue that the effective limit is not

	m_0= 172. GeV/c^2 $\tan\beta$= 1.5 M_2=150. GeV/c^2 $\mu = -150.\ GeV/c^2$ Mass $\chi_1^{\pm}$= 154 GeV	m_0= 172. GeV/c^2 $\tan\beta$= 1.5 M_2=800. GeV/c^2 $\mu = 150.\ GeV/c^2$ Mass $\chi_1^{\pm}$= 140 GeV	m_0= 172. GeV/c^2 $\tan\beta$= 1.5 M_2=250. GeV/c^2 $\mu = -100.\ GeV/c^2$ Mass $\chi_1^{\pm}$= 115 GeV
efficiency	52%	44%	51%
σ_{lim} *upper limit at 95%CL*	$1.3pb$	$1.3pb$	$1.0pb$
λ_{121} *upper limit at 95%CL*	0.005	0.007	0.003

Table 14: Efficiencies, model-independent σ_{lim} and λ_{121} upper limits at 95 % CL for the signal.

too much model dependent.

In conclusion, DELPHI data allow to set a very tight constraint (λ at a few 10^{-3})on R-parity violation in the leptonic sector if there is a sneutrino with mass below 172 GeV. This result survives if, as assumed in [32], the sneutrino couples to b$\bar{b}$ final states.

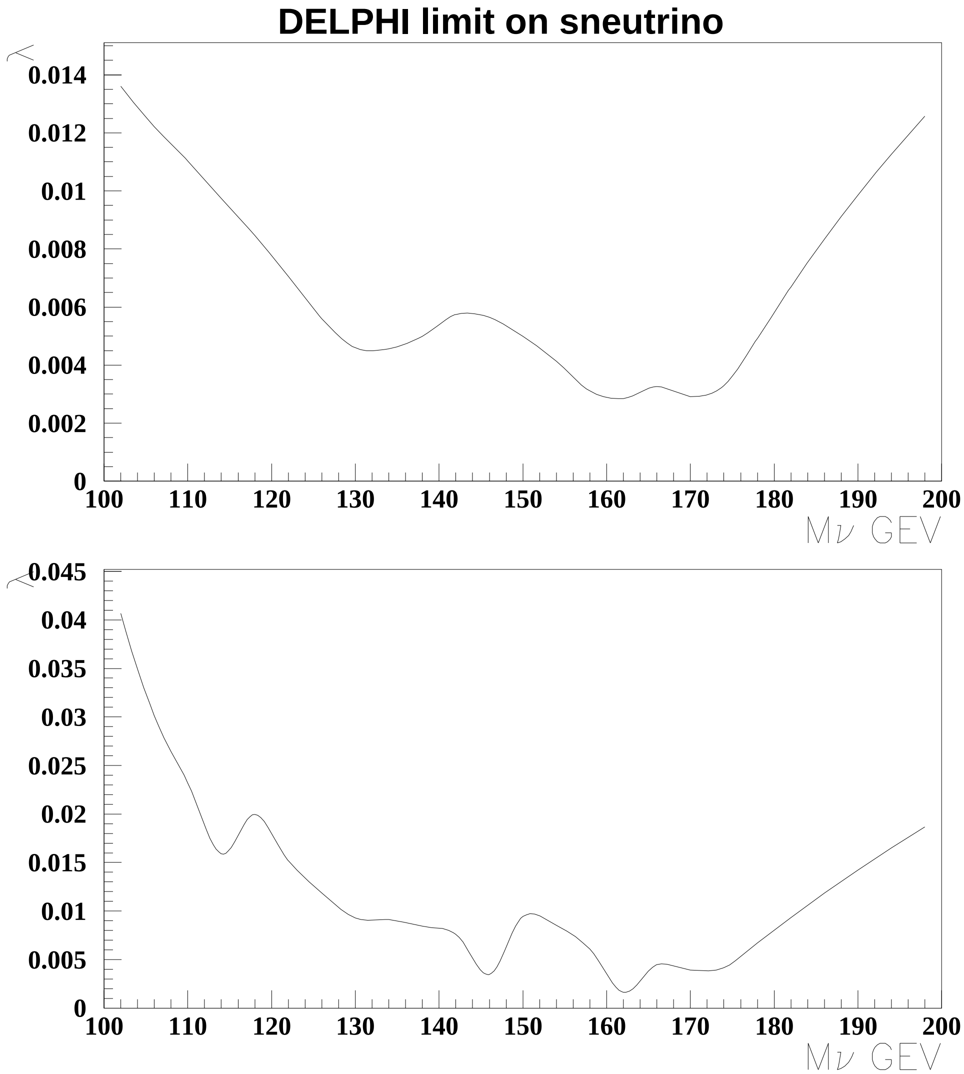

Figure 14: The upper curve corresponds to the limit on the coupling of $e^+e^- \to \tilde{\nu}$ assuming that the sneutrino decays into $\chi\nu$ with $\chi \to e^+e^-\nu$ and that DELPHI searches have a 50 % efficiency on this channel. The lower curve corresponds to the DELPHI limit when the process $e^+e^- \to \tilde{\nu} \to b\bar{b}$ becomes dominant. $\Gamma_{\tilde{\nu}}$=8 GeV was assumed.

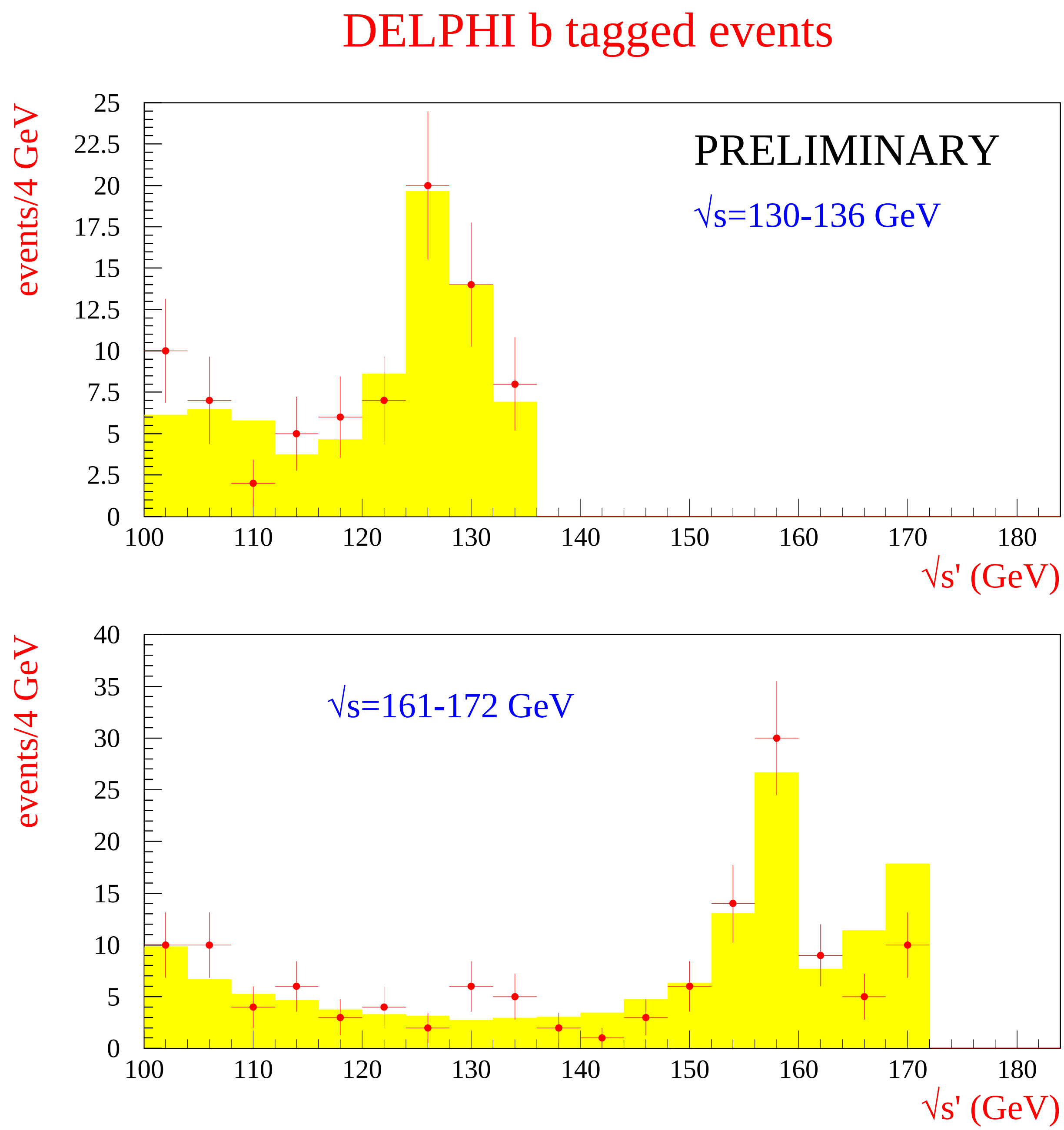

Figure 15: Mass distribution observed for b-tagged Delphi events

Energy GeV	ADLO pb	ZFITTER pb	low . lim. pb	upper lim. pb
161	36.7 $\pm$ 1.1	35.1	-0.2	3.4
170+172	30.0 $\pm$ 1.1	29.1	-0.9	2.7

Table 15: Combined LEP2 results on hadronic cross sections

7 Indirect effects: sparticle exchange in the t channel

Assuming R-parity non conservation with lepton number violation (λ' term), an effect can be induced at LEP2 on $e^+e^- \to q\bar{q}$ processes through a t-channel exchange of an up or down type squark. Cross sections and charge asymmetries measurements of the various quark flavors can therefore provide an indirect evidence of the existence of heavy squarks. The formulae used to estimate these effects are described in [14] and have been cross-checked using results of [51]. Experimental results are based on an analysis using Delphi data collected at 130-136, 161 and 172 GeV which is described in [48].

7.1 Effect on the total hadronic cross-section

A negative interference is expected between the squark exchange amplitude and the SM amplitude with the relevant helicities [14]. When a down-type squark is exchanged ($u\bar{u}$ and $c\bar{c}$ final states) , the effect is maximal since the interference occurs with a large SM term. In contrast, for an up-type squark exchange ($d\bar{d}$, $s\bar{s}$ and $b\bar{b}$ final states) , the interference term becomes negligible which considerably reduces the sensitivity of the measurement.

Combining the 4 LEP experiments [49], one can derive the upper limits (95% C.L.) shown in table 15. These cross sections have been obtained selecting events with more than 85% of the center of mass energy. Assuming that there is no other source of deviation (e.g. Z', contact terms) to the standard model than the contribution of a given squark to a given flavor channel, one derives the limits of figure 16 and 17.

The sensitivity of these results is excellent when a down-type squark is exchanged and is sufficient to exclude this hypothesis for the effect seen at HERA [50]. As explained in [14], one can estimate from the HERA effect that λ' should be $\sim$0.40/$\sqrt{Bf}$, where Bf is the branching ratio of the squark into e^+q. B_f $\sim$0.5 since down-squarks can decay into d+ν (R-parity conserving channels should not influence too much B_f given the large value assumed for λ').

When an up-squark is exchanged, the sensitivity is reduced as can be seen in figure 17 but is not far from constraining a scenario for which the HERA effect would be due to an s quark from the sea. λ' $\sim$0.06/$\sqrt{Bf}$ if the process seen at HERA is e^+d $\to \tilde{u_L}$. Given this low value, R-parity conserving processes could contribute and one can assume [26] that B_f varies from 0.1 to 1. If the HERA process is e^+s $\to \tilde{u_L}$, λ' $\sim$0.40/$\sqrt{Bf}$ and one therefore expects B_f $\sim$1.

7.2 Effect on separate flavors

As explained in reference [48], flavor separation between b, c and light quarks is obtained using the vertex informations with the purities/efficiencies given in table 16.

Cross-sections and charge asymmetry (jet charge measurements) can therefore be derived for these flavors. Results are summarized in table 17. The cross sections ratios R_q, defined as the

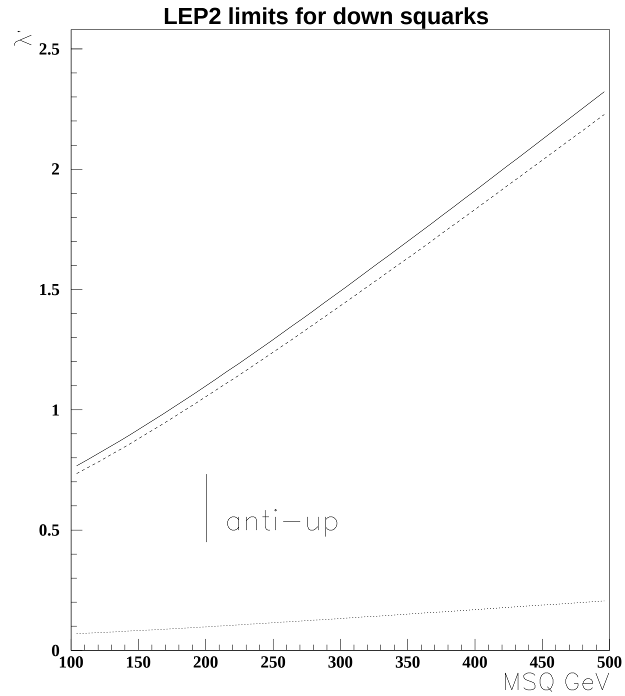

Figure 16: The curve shows the 95% C.L. limit obtained from LEP2 rates. The vertical bar shows the prediction from HERA assuming that the squark is produced from an anti-up quark from the sea. In the region between the dotted curve and the dashed curve the interference term dominates and gives a negative effect which can be rejected at the 95% C.L. by the rates measured at the LEP2. Between the dashed curve and the full curve, there is a blind zone for LEP2. Above the full curve there would be a positive effect which can also be rejected at the 95% C.L. by the rates measured at the LEP2.

ratio of the cross section for one quark flavor to the total hadronic cross section, and forward-backward asymmetries for bottom, charm and light quark events are compared to the Standard Model expectations. No significant deviations from the Standard Model expectations are found. These measurements can be interpreted in terms of an upper limit on the λ' couplings. Figure 18 shows the limits obtained from the $b\bar{b}$ final states. Note that these limits are derived assuming that there is no other source of deviation to the standard model than the contribution of an up squark to the $b\bar{b}$ channel.

As discussed in [14] and [51], for an up-type squark exchange there is anti-correlation between A_{FB} and the cross-section changes. This should allow to verify, in case of a significant deviation, the consistency of the overall result with the squark hypothesis. This is illustrated in figure 19.

For the $c\bar{c}$ final states one observes a 2.5σ deviation on the charge asymmetry w.r.t. to the the SM but this effect does not match with the prediction from a down-type squark exchange as shown in figure 20.

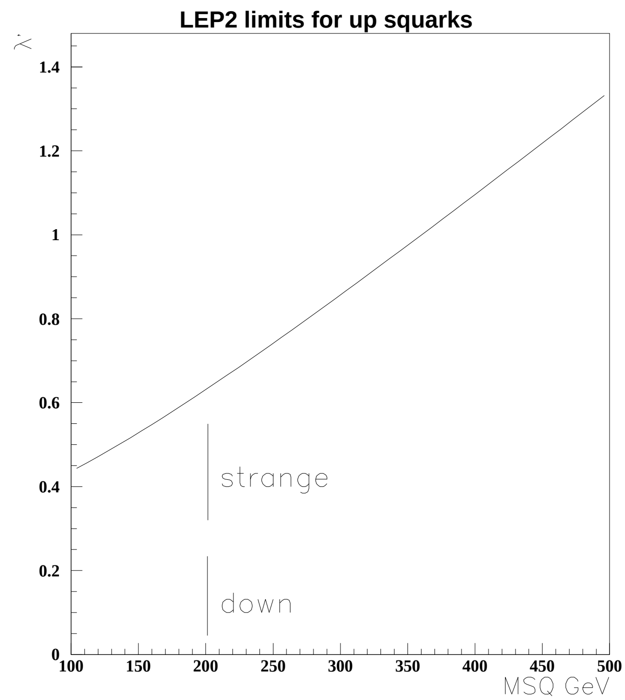

Figure 17: The curve shows the 95% C.L. limit obtained from LEP2 rates. The vertical bars show the prediction from HERA if the squark is produced from a down valence quark or from a strange quark from the sea. The length of the bars reflect the measurement uncertainty. For the down valence quark case, it also includes the uncertainty due to R-parity allowed decay modes as explained in the text.

tag	efficiency	b purity	c purity	uds purity
bottom	0.67 (b)	0.77	0.18	0.05
charm	0.33 (c)	0.17	0.40	0.43
light quark	0.76 (uds)	0.03	0.23	0.74

Table 16: Efficiencies and purities (in %) for the different tags at energies of 161-172 GeV selecting events with more than 85% of the center of mass energy.

quark flavor (energy)	$(R_q - R^{SM})/R^{SM}$	total error	$A^q_{fb} - A^{SM}_{fb}$	total error
bottom (130-136 GeV)	-0.17	0.17	0.21	0.52
charm (130-136 GeV)	-0.26	0.33	-0.75	1.2
light (130-136 GeV)	0.11	0.10		
down (130-136 GeV)	0.34	0.31	0.95	0.65
up (130-136 GeV)	0.26	0.24	-0.75	0.52
strange (130-136 GeV)	0.38	0.35	0.78	0.54
bottom (161-172 GeV)	-0.13	0.15	0.02	0.41
charm (161-172 GeV)	-0.05	0.25	-1.91	0.78
light (161-172 GeV)	0.05	0.08		
down (161-172 GeV)	0.16	0.26	-1.19	0.62
up (161-172 GeV)	0.12	0.20	0.75	0.39
strange (161-172 GeV)	0.18	0.29	-1.25	0.64

Table 17: The derived quark cross section ratio and forward-backward quark asymmetry difference w.r.t the Standard Model for different flavors at energies of 130-136 and 161-172 GeV selecting events with more than 85% of the center of mass energy.

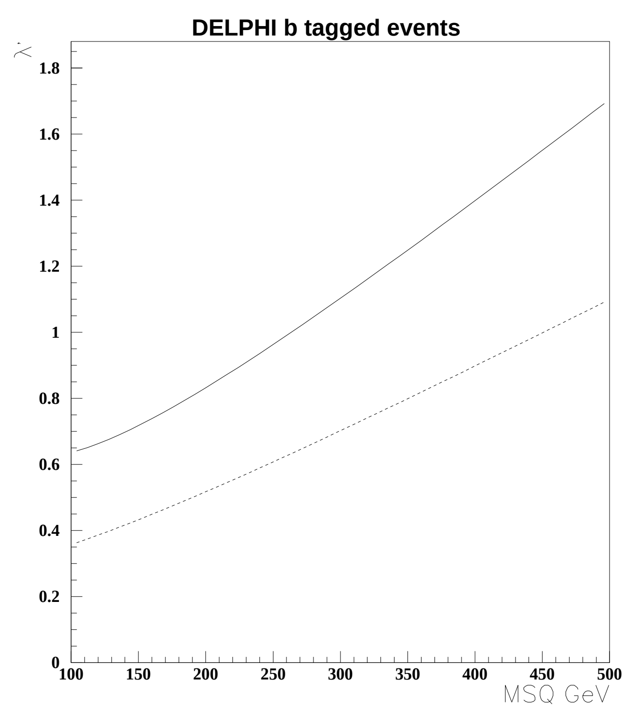

Figure 18: The curve shows the 95% C.L. limit obtained from charge asymmetry and from rates (dashed curve) on b-quarks with DELPHI data.

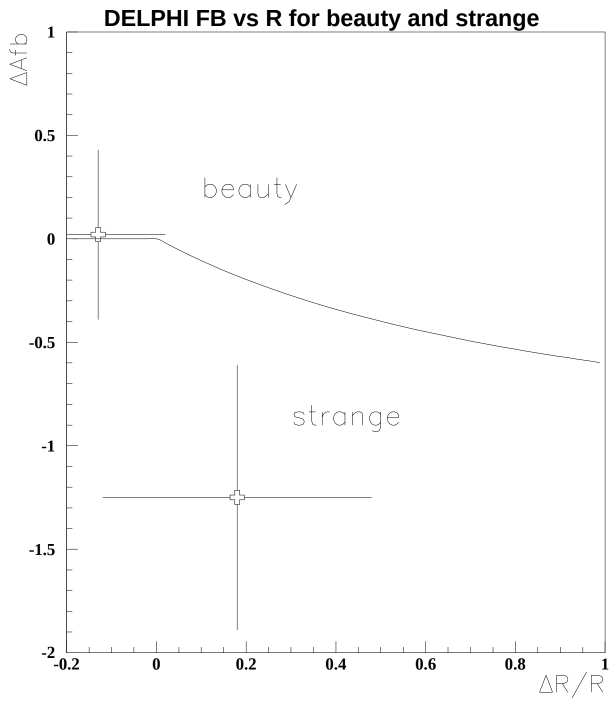

Figure 19: The curve shows the correlation between the variation of the b charge asymmetry and that of the ratio Rb. The DELPHI measurement is indicated for beauty and strangeness. A mass of 200 GeV is assumed for the squark.

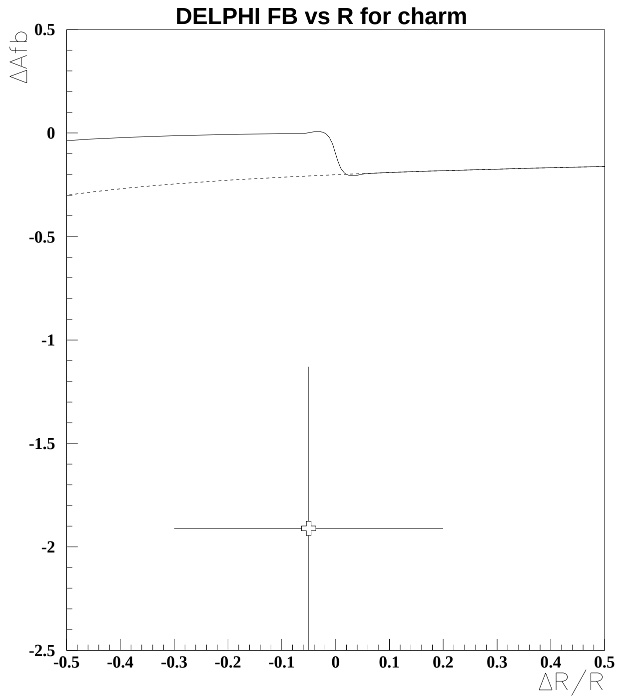

Figure 20: The curve shows the correlation between charge asymmetry and R for charm quarks assuming a 200 GeV squark. The cross corresponds to the DELPHI measurement.

With present accuracies, t-channel effects in the leptonic sector will not provide strong constraints on sneutrino couplings.

7.3 Results

In conclusion:

- The interpretation of the HERA effect as due to $\tilde{d}_R$ is excluded by the hadronic cross-sections measured at LEP2.
- The interpretation of the HERA effect as due to $\tilde{t}_L$ cannot be confirmed by LEP2 data unless $\tilde{t}_L$ couples preferentially to s or b quarks. No significant effect is observed in these channels using the DELPHI data.
- If, with more data, a rate effect is seen at LEP2 in s$\bar{s}$ or b$\bar{b}$ final states, the charge asymmetry will help in confirming the squark hypothesis.

8 Complementarity of the searches

Figure 21 presents a synopsis of the complementary searches and measurements that can be performed in an e^+e^- collider, and in particular at DELPHI. There can be 2 possible intrrepretations of the HERA anomalous events as squark production through the R-Parity violating operator λ'. Production of a left up squark from a valence d

$$e^+d \rightarrow \tilde{c}_L, \tilde{t}_L(\lambda'_{121}, \lambda'_{131}) \tag{7}$$

Production of a left up squark from a sea s, or right down quark from a sea anti-up quark.

$$e^+s \rightarrow \tilde{c}_L, \tilde{t}_L(\lambda'_{122}, \lambda'_{132}) \tag{8}$$

$$e^+\bar{u} \rightarrow \tilde{s}_R, \tilde{b}_R(\lambda'_{121}, \lambda'_{131}) \tag{9}$$

As we have shown in the previous sections, we can look for an equivalent effect at LEP in 3 ways:

- Pair production: The λ' operators do not affect the production cross-section, since it is a R-Parity conserving one. They only determine the decay properties. Depending on the strength of λ' the direct R-Parity violating decays can dominate or not over the cascade decays. The stop case is a particular one, since its R-Parity conserving decay is naturally supressed when the stop is below the top, and it occurs mostly through a Cabibo-Kobayashi-Maskawa transition to charm and the neutralino. The direct R-Parity violating decays dominate down to a strength of 10^{-4}. The search of the stop described in section 4 in the 2 lepton + 2 jets channel provides the limit extending down to very low λ'. This corresponds to the dark area in the upper plot. Unfortunately the right sbottom is produced with a very small cros-section at LEP and the indirect decays dominate, so a more complete analysis has to be implemented. For the time being no limit can be reported.

- Single production: The squarks can be produced singly as shown in section 6 through an emitted gamma "resolved" to a quark-antiquark pair. Here the study looking for a leptoquark decaying in a charged lepton + jet in DELPHI can be transposed in a supersymmetric context. Since for the stop the direct decays dominate for the λ' above 10^{-4} and the only possible decay is $\tilde{t} \rightarrow eq$, the leptoquark limits for a production of a charge 2/3 scalar, with branching ratio 1, are reported in light grey in the same plot. For the sbottom case, two direct possible decays are open $\tilde{b} \rightarrow eq$ ou $\tilde{b} \rightarrow \nu q$, since our search was only in the lepton + jet channel, we take the branching ratio 50% limits of the leptoquark paper. The supersymmetric R-Parity decays will worsen this picture unless an indirect search is done, but since anyway this search is less sensitive than the t channel limits, we do not pursue the matter further.

- Exchange of a squark in the t channel: Further the indirect decays are reported on the same plot in medium dark colour. The idirect search barely touches the s interpretation of the anomalous events, while completely excludes the $\bar{u}$ interpretation. The H1 stop exclusion (in blue) while it seems to exclude the s interpretation, it had assumed a valence quark, so it is not immediately applicable.

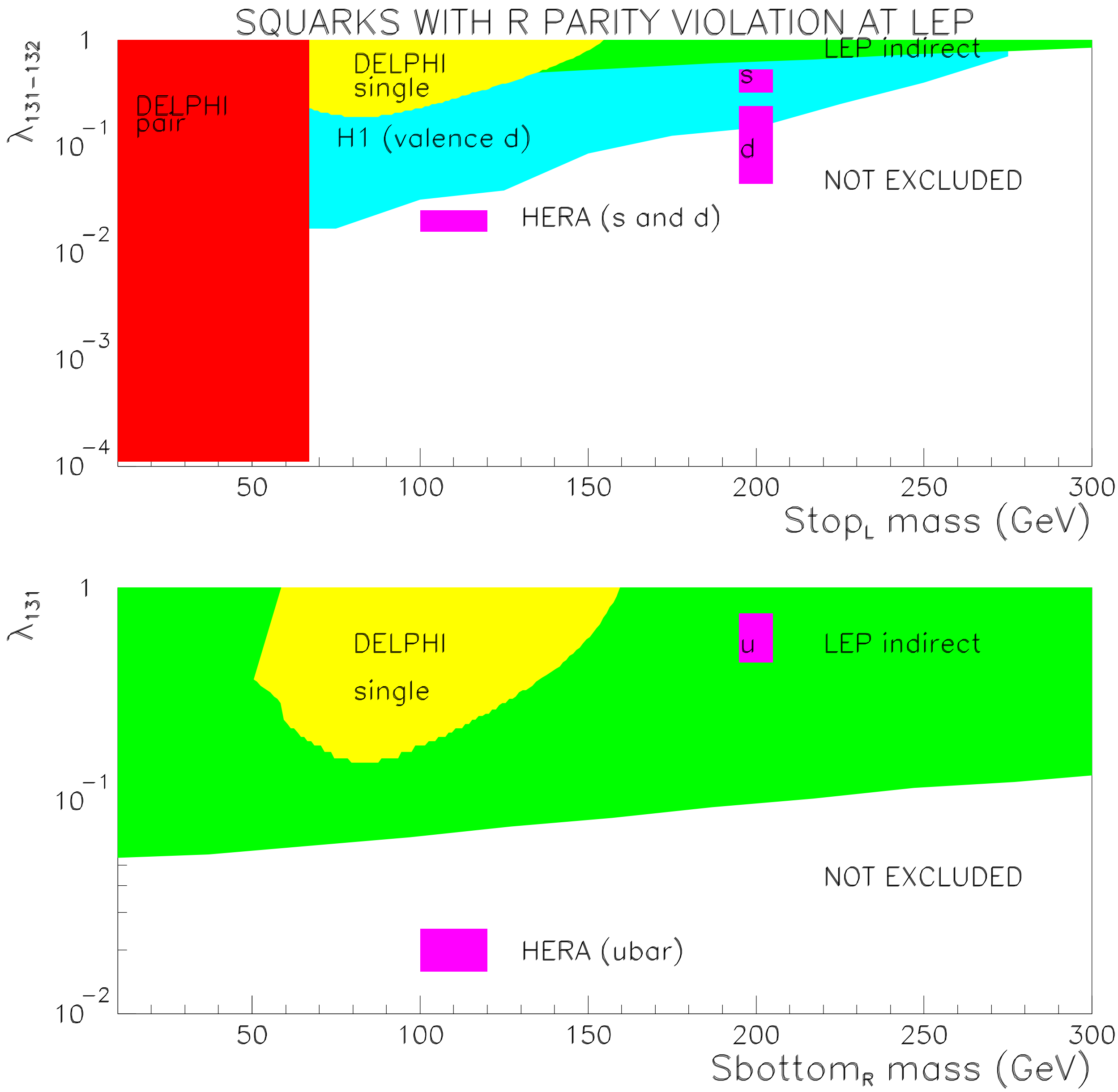

Figure 21: Exclusion domain in the λ' versus $m_{\tilde{q}}$ plane.

9 Conclusions

In this paper, preliminary results are shown on the possible manifestations of R-Parity violation at an e^+e^- collider, using the DELPHI detector. Three main categories of effects were investigated, pair production of sparticles, single production of sparticles and indirect effects through exchange of sparticles in the t channel.

The first category of effects, pair production of sparticles, not depending on the $\not{R}_p$ couplings λ can probe these same couplings till the limit of the sparticle decaying beyond the fiducial volume of the detector, turning an $\not{R}_p$ search to an R_p one. The possible signatures are varied, ranging from $\not{R}_p$ specific signatures as e.g multileptons examined in section 3, and multijets examined in section 6, through signatures common with other searches, e.g 4 jets, 2 jets and 2 leptons as in Higgs searches, where nevertheless specific strategies have to be developed, to signatures where one can with a minimal effort transpose results from R_p searches, as for example the acoplanar leptons and jets, in common with slepton and squark studies. We have presented prototype studies for searches of neutralinos and charginos decaying through the purely leptonic or purely hadronic operators. Exclusion plots in the MSSM plane at 95% are shown for a typical such operator in figure 6. The inclusion in the future of indirect or cascade decays, resulting very often in mixed leptonic and hadronic topologies will make these searches model independent. In the sfermion sector we have presented a series of new limits, on sneutrinos, selectrons, stops and sbottoms, under the assumption that these sparticles are the LSP and therefore indirect decays are not relevant. The independence from this assumption has been partially explored in the case of a sneutrino decaying leptonically. Further, in the case of the stop the naturally suppressed R_p decay width permits the study of λ couplings down to $\sim 10^{-4}$ independently of this assumption. On all sfermion cases we have studied 2 characteristic decay operators, e.g λ and λ' for sleptons and λ' and λ'' for squarks. The single sfermion production and the exchange of squarks in the t channel is a means to extend the study of sfermions beyond the double production kinematical limit, though one has to pay the price of loosing the quasi-independence from the strength of λ's, as can be seen in figure 21.

Finally, the studies presented in this paper intend to show that the complementarity of signatures and modes of production at LEP makes the search of $\not{R}_p$ effects, a finite and well defined task despite the 45 new couplings that $\not{R}_p$ models introduce.

Acknowledgements

We are greatly indebted to our technical collaborators and to the funding agencies for their support in building and operating the DELPHI detector. Very special thanks are due to the members of the CERN-SL Division for the excellent performance of the LEP collider.

References

[1] H.P. Nilles, Phys. Rep. **110** (1984) 1;
H.E. Haber and G.L. Kane, Phys. Rep. **117** (1985) 75.

[2] P. Fayet, Phys. Lett. B69 (1977) 489; G.R. Farrar and P. Fayet, Phys. Lett. B76 (1978) 575.

[3] Search for charginos and neutralinos with R-Parity violation at $\sqrt{s}$ 130 and 136 GeV, ALEPH, Phys. Lett. B384(1996)461. Search for supersymmetric particles with R-Parity violation in Z decays, ALEPH, Phys. Lett. B349(1995)238

[4] L. E. Ibanez and G. G. Ross, Phys. Lett. B 260 (1991) 291; L.E.Ibanez and G.G.Ross, Nucl. Phys. B368 (1992) 3; S. Lola and G.G. Ross, Phys. Lett. B314 (1993) 336; H. Dreiner and A. Chamseddine, Nucl. Phys. B 458 (1996) 65; K. Tamvakis, Phys. Lett. B383 (1996) 307; Phys. Lett. B382 (1996) 251.

[5] V.Barger, G.F.Giudice and T.Han, Physical Review D40(1989)2987.

[6] For a review on the limits of R-parity violating couplings, see G. Bhattacharyya, Nucl.Phys.Proc.Suppl.52A (1977) 83-88 and references therein; Also: Supersymmetry 1996, Theoretical perspectives and experimental outlook, Nuclear Physics B(proc.suppl)52A(1997), Proceedings of the 28th International conference on high energy physics, Z.Ajduk and A.K.Wroblewski editors, World Scientific (1997), M.Hirsch, H.V.Klapdor-Kleingrothaus and S.G.Kovalenko, Physical Review letters, 75(1995),17, G.Bhattacharyya and D.Choudhury, hep-ph/9503263, G.Bhattacharyya, J.Ellis and K.Sridhar, hep-ph/9503264, G.Bhattacharyya, hep-ph/9511447, M.Hirsch, H.V.Klapdor-Kleingrothaus and S.G.Kovalenko, hep-ph/9512237, G.Bhattacharyya and A.Raychaudhuri, hep-ph/9512277, D.K.Ghosh, S.A.Raychaudhuri and K.Sridhar, hep-ph/9608352, J.H.Jang, Y.G.Kim and J.S.Lee, hep-ph/9704213; K. Agashe and M. Graesser, Phys. Rev. D54 (1995) 4445; A. Deandrea, hep-ph/9705435; L. Giusti and A. Strumia, hep-ph/9706298.

[7] B. Campbell, S. Davidson, J. Ellis, and K.A. Olive, Phys. Lett. **B256** (1991) 457;
W. Fischler, G.F. Giudice, R.G. Leigh, and S. Paban, Phys. Lett. **B258** (1991) 45.

[8] See, *e.g.*, A.G. Cohen, D.B. Kaplan, and A.E. Nelson, *Ann. Rev. Nucl. Part. Sci.* **43** (1993) 27;
V.A. Rubakov and M.E. Shaposhnikov, *Phys. Usp.* **39** (1996) 461, and references therein.

[9] L.J.Hall and M.Suzuki, Nucl. Phys. B231(1984)419.

[10] S.Dawson, Nuclear Physics B261(1985)297.

[11] J. Ellis et al., Phys.Lett. B150 (1985) 142; G.G. Ross and J.W.F. Valle, Phys.Lett. B151 (1985) 375; S. Dimopoulos and L.J. Hall, Phys. Lett. B207 (1988) 210; S. Dimopoulos, R. Esmaizadeh, L. Hall and G. Starkman, Phys. Rev. D 41, 2099 (1990); H. Dreiner and G. G. Ross, Nucl. Phys. B365 (1991) 597; S. Lola and J. Mccurry, Nucl. Phys. B381 (1992) 559.

[12] C. Papadopoulos, hep-ph/9703372.

[13] H. Dreiner and S. Lola, DESY 96-123D (1996) 435.

[14] Possible implications at LEP2 of the effect seen at HERA DELPHI 97-46 PHYS 698 by F. Richard (May 1997).

[15] J. Kalinowski et al. DESY 97-044, March 1997.

[16] M. Doncheski and S. Godfrey, Phys. Lett. **B393** (1997) 355.

[17] DELPHI Coll., P. Aarnio *et al.*, Nucl. Instr. and Meth. **303** (1991) 233;
DELPHI Coll., P. Abreu *et al.*, Nucl. Instr. and Meth. **378** (1996) 57.

[18] SGV 1.0 Simulation à Grande Vitesse, M. Berggren, P. Billoir and M. A. Do Vale, unpublished.

[19] T. Sjöstrand, Comp. Phys. Comm. **39** (1986) 347; T. Sjöstrand, `PYTHIA 5.6` *and* `JETSET 7.3`, CERN-TH/6488-92.

[20] F.A. Berends, R. Pittau, R. Kleiss, Comp. Phys. Comm. **85** (1995) 437.

[21] S. Nova, A. Olshevski, and T. Todorov, *A Monte Carlo event generator for two photon physics*, DELPHI note 90-35 (1990).

[22] F.A. Berends, P.H. Daverveldt, R. Kleiss, Comp. Phys. Comm. **40** (1986) 271, Comp. Phys. Comm. **40** (1986) 285, Comp. Phys. Comm. **40** (1986) 309.

[23] SUSYGEN 2.17 S. Katsanevas and P. Morawitz in preparation (Imperial and IPNLyon notes, web site http://lyohp5.in2p3.fr//delphi/katsan/susygen.html) and SUSYGEN S. Katsanevas and S. Melachroinos Physics at LEP2 CERN 96-01 Vol. 2. p. 328.

[24] V.Barger, G.F. Guidice, T. Han Phys. Rev. D40 (1989) 2987.

[25] G.Bhattacharyya Nucl. Phys. B (Proc. Suppl.) 52A (1997) 83.

[26] HEP'97 353 Search for Sfermions at $\sqrt{s}$ = 161 and 172 GeV DELPHI Jerusalem 97, pa 11, 13 pl 9, 15, 17

[27] Particle Data Group. Phys. Rev. D 54.1 (1996)

[28] T.Kon, T. Kobayashi and S.Kitamura, ITP-SU-94/01.

[29] K. Hikasa and M.Kobayashi, Physical Review D36(1987)724.

[30] M.Besançon and Ph.Gris, Delphi 96 PHYS 600.

[31] P.Gris Delphi note 97-54 PHYS 704.

[32] V. Barger et al., Proceedings of SUSY '96, Nucl. Phys. B52A (1997) p. 89.

[33] L.J.Hall and M.Suzuki, Nucl. Phys. B231(1984)419. H.P. Nilles and N.Polonsky hep-ph/9606388. N.Polonsky hep-ph/9612397. A.Y. Smirnov and F. Vissani, Nucl.Phys. B460(1996)37

[34] M.Drees and K.I.Hikasa, Scalar top production in e^+e^- annihilation, Physics Letters 252B(1990)127.

[35] S.Kawabata, A new Monte Carlo event generator for high energy physics, Computer Physics Communication 41(1986)127.

[36] M.Jimbo, T.Kaneko and T.Kon, MINAMI-TATEYA collaboration, , The Susy-Grace system, TMCP-95-1.

[37] Search for neutral and charged Higgs bosons in e^+e^- collisions at 161 and 172 GeV, Delphi 97-22 PHYS 678 and CERN PPE preprint in preparation.

[38] S. Catani et al., Phys. Lett. **B269** (1991) 432.

[39] A. Duperrin a multijet rescaling algorithm, DELPHI note in preparation.

[40] DELPHI 91-17 Phys 88, Reconstruction of Invariant Masses in Multi-jet Events, N.J.Kjaer, R.Moller.

[41] DELPHI 97-0 XXXX 000, Multijets HZ and hA analysis with the DELPHI detector at the center of mass energy of 161 and 172 GeV, P.Bambade et al.

[42] Cavendish-HEP-95/15, Perturbative rates and colour rearrangement effects in four jet events at LEP200, A. Ballestrero et al.

[43] AABTAG, AACMHA programs, GV. Borisov. DELPHI 97-16 Phys 672, Performance of b tagging at LEP2, G.V.Borisov, C.Marioti.

[44] Search for Leptoquarks at $\sqrt{s}$ = 161 and 172 GeV DELPHI Jerusalem 97, pa 11, 13 pl 9, 15, 17

[45] M. Doncheski and S. Godfrey, Phys. Rev. **D49** (1994) 6220.

[46] M. Gluck et al., Phys.Rev. **D46** 1973 (1992) and Phys.Rev. **D45** 3986 (1992).

[47] DELPHI Coll., P. Abreu et al., Phys. Lett. **B393** (1997) 245.

[48] A measurement of the cross sections and asymmetries for flavour tagged events at 161 and 172 GeV and limits on new interactions. DELPHI 97-47 PHYS 699 by P. Kluit (April 1997).

[49] D.Gele, proceedings of the EW session of Moriond 1997.

[50] Observation of events at very high Q^2 in e p collisions at HERA. By H1 Collaboration (C. Adloff et al.). DESY-97-024, Feb 1997. Submitted to Z.Phys.C and Comparison of ZEUS Data with Standard Model Predictions for e+p→ e+X Scattering at High x and Q-squared. DESY Preprint No 97-025. Submitted to Z. Phys. C

[51] G. Altarelli et al., CERN-TH/97-40, March 1997,hep-ph/9703436. H. Dreiner and P. Morawitz, hep-ph/9703279. J. Kalinowski, R.Rückl, H. Spiesberger and P. M. Zerwas BI-TP 97/07, DESY 97-038, WUE-ITP-97-02,hep-ph/9703288. J. Ellis, S. Lola and K. Sridhar, CERN-TH-97-109. hep-ph/9706519